Identification of chalcone-based antileishmanial agents targeting trypanothione reductase

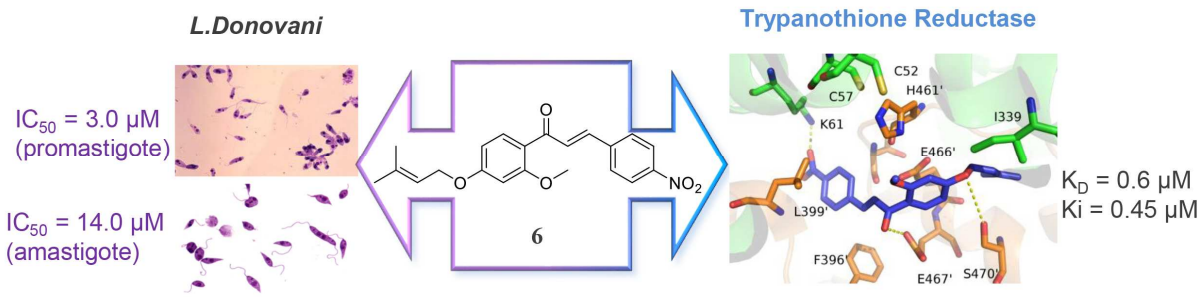
L.Donovani
Trypanothione Reductase
IC50 = 3.0 μM
(promastigote)
IC50 = 14.0 μM
(amastigote)
O
O
O
NO2
6
C52
C57
H461'
K61
I339
E466'
L399'
F396'
E467'
S470'
KD = 0.6 μM
Ki = 0.45 μM

Identification of Chalcone-based Antileishmanial Agents Targeting Trypanothione Reductase

Margherita Ortalli[1], Andrea Ilari[2], Gianni Colotti[2], Ilenia De Ionna[3], Theo Battista[3], Alessandra Bisi[4], Silvia Gobbi[4], Angela Rampa[4], Rita M. C. Di Martino[4§], Giovanna A. Gentilomi[4], Stefania Varani[1,5]^ and Federica Belluti[4]^*

[1]*Department of Experimental, Diagnostic and Specialty Medicine, Alma Mater Studiorum University of Bologna, Bologna, Italy*

[2]*CNR-Institute of Molecular Biology and Pathology, Rome, Italy*

[3]*Department of Biochemical Sciences "A. Rossi Fanelli", Sapienza University, Rome, Italy*

[4]*Department of Pharmacy and Biotechnology, Alma Mater Studiorum University of Bologna, Bologna, Italy.* [§] *Present address: Department. of Drug Discovery and Development, Istituto Italiano di Tecnologia,via Morego n.30, 16163 Genova, Italy*

[5]*Unit of Clinical Microbiology, Regional Reference Centre for Microbiological Emergencies (CRREM), St. Orsola-Malpighi University Hospital, Bologna, Italy*

^ these authors contributed equally to this work

*Corresponding author: federica.belluti@unibo.it

Abstract

All currently used first-line and second-line drugs for the treatment of leishmaniasis exhibit several drawbacks including toxicity, high costs and route of administration. Furthermore, some drugs are associated with the emergence of drug resistance. Thus, the development of new treatments for leishmaniasis is a priority in the field of neglected tropical diseases. The present work highlights the

use of natural derived products, i.e. chalcones, as potential source of antileishmanial agents. Thirty-one novel chalcone compounds have been synthesized and their activity has been evaluated against promastigotes of *Leishmania donovani*; 16 compounds resulted active against *L. donovani* in a range from 3.0 to 21.5 μM, showing low toxicity against mammalian cells. Among these molecules, **6** and **16** showed good inhibitory activity on both promastigotes and intracellular amastigotes, coupled with an high selectivity index. Furthermore, compounds **6** and **16** inhibited the promastigote growth of other leishmanial species, including *L. tropica*, *L. major* and *L. infantum*. Finally, **6** and **16** interacted with high affinity with trypanothione reductase (TR), an essential enzyme for the leishmanial parasite and compound **6** inhibited TR with sub-micromolar potency. Thus, the effective inhibitory activity against *Leishmania*, the lack of toxicity on mammalian cells and the ability to block a crucial parasite's enzyme, highlight the potential for compound **6** to be optimized as novel drug candidate against leishmaniasis.

Keywords

Chalcone, drug discovery, leishmaniasis, natural products, neglected tropical disease, trypanothione reductase

1. INTRODUCTION

Leishmaniases are vector-borne infections caused by protozoan parasites belonging to the genus *Leishmania* that are transmitted through the bite of phlebotomine sand flies of the genus *Phlebotomus* in the Old World [1]. Most forms of the diseases are zoonotic and only 21 of the 30 *Leishmania* species that infect mammals may cause human infection.

Most infections caused by *Leishmania* parasites are asymptomatic, but in symptomatic patients clinical manifestations range from cutaneous leishmaniasis (CL), which may result in disfiguring

scars if left untreated, to the potentially fatal visceral leishmaniasis (VL), which is characterized by fever, splenomegaly, pancytopenia and weight loss [2].

Leishmaniases are distributed in Asia, Africa, Latin America and Southern Europe, with an estimation of 1.5-2.0 million new cases per year of CL and 0.5 million cases of VL [3]. Despite this, leishmaniases are classified among the most neglected diseases, based on their strong association with poverty and on the limited resources invested in their diagnosis, treatment and control [2]. Chemotherapy is the only method for protection against leishmaniasis, since there is currently no approved vaccine for humans [4]. Treatment of leishmaniasis comprises liposomal amphotericin B, pentavalent antimonials, paromomycin and miltefosine; these drugs are plagued by several limitations including high costs, toxicity, route of administration and poor efficacy [5]. Moreover, the increasing emergence of *Leishmania* parasites that are resistant to antimonial drugs is a serious problem in several endemic regions [6]. This scenario emphasizes the need of developing novel effective, safe and economically feasible antileishmanial agents.

The implementation of the genome project for many trypanosomatid species lead to the identification of several drug targets suitable for gaining parasite selective inhibition [7]. Indeed, targeting a unique and essential parasite metabolic pathway, which is absent in mammals is generally considered a successful therapeutic strategy.

In this context, the thiol-dependent redox polyamine metabolism represents an essential detoxifying system by means of which the parasite eliminates its toxic endogenous metabolites [8]. While the mammalian redox defense machinery is based on glutathione (GSH), the protozoan parasites from the Trypanosomatidae family, including *Trypanosoma* and *Leishmania,* strictly depend on a different pathway for supporting their intracellular redox homeostasis; they employ trypanothione (*N1,N8*-bis–glutathionyl-spermidine) in its reduced thiol form $T(SH)_2$ [9]. Trypanothione disulfide (TS_2) is obtained by means of two consecutive steps, each involving the conjugation of GSH to N_1 and N_8 amino groups of spermidine by the ATP-dependent C-N ligase trypanothione synthetase (TryS). Trypanothione reductase (TR), a NADPH-dependent flavoprotein,

reduces TS_2 to $T(SH)_2$, thus ensuring an intracellular reducing environment. The inhibition of TryS and/or TR is known to disrupt the parasite redox balance [10, 11]; these two enzymes can be regarded as validated molecular targets for the development of effective and selective antileishmanial drugs [9, 12].

TR inhibition may be achieved by competing with trypanothione binding to the active site; for example, trivalent antimony Sb(III), the active form of the antimonial drug sodium stibogluconate (SSG) [13], a number of metals, such as Ag(I) and Au(I) [14-16] and some TR inhibitors, such as azole and diaryl compounds [17, 18] have been reported to directly bind the trypanothione binding site.

Natural products (NPs) including flavonoids, isoflavonoids, saponins, alkaloids, tannins and indoles have been shown to exert antileishmanial effects [19, 20]. Among them, chalcones (1,3-diaryl-2-propen-1-ones), prominent secondary metabolites and precursors of flavonoids, can be considered "privileged structures", i.e. evolutionary-chosen molecules that have evolved to achieve an inherent affinity for diverse biological macromolecules in the natural selection process [21]. Indeed, chalcones display a wide range of pharmacological effects, including antioxidant, antimutagenic, antimitotic, antimetastatic and antiinflammatory activity [22, 23]. The antileishmanial potential of chalcones has also been demonstrated [20]; naturally occurring chalcones such as licochalcone A and isocordoin (Figure 1), isolated from *Glycyrrhiza glabra* and *Lonchocarpus xuul*, respectively, were able to efficiently inhibit the proliferation of different *Leishmania* species [24-26]. Unfortunately, the intrinsic cytotoxicity of these molecules may represent an undesired aspect**.** In this study, the chalcone framework was selected as main scaffold to develop a new series of effective and safe antileishmanial agents and targeting a key enzyme in the polyamine-trypanothione pathway, ie TR.

Therefore, we have synthesized 31 novel chalcones, evaluated their activity against *Leishmania* vs. mammalian cells and tested both interaction and ability to inhibit *L. donovani* TR.

2. RESULTS

2.1 Design strategy

A small library of 31 chalcone-based analogues was designed and synthesized (Figure 1). In particular, the A-ring of the main scaffold was properly functionalized at the positions 2 and 4: the C-4 position was occupied by a suitable alkoxy function (O-R), namely 3,3-dimethylallyoxy (or prenyloxy) and propargyloxy affording Series 1 and 2, respectively. The C-2 position was differently functionalized by introduction of hydroxy, methoxy, prenyloxy and propargyloxy groups (O-R_1). In order to perform a Structure Activity Relationship (SAR) study, different moieties were introduced as B-ring, namely pyridine or aryl functions bearing methoxy, bromo, nitro, and fluorine substituents.

2.2. *Synthesis*

All the tested chalcones were readily synthesized through the classic base-catalyzed Claisen-Schmidt procedure (as shown in Scheme 1). In details, the selected acetophenone was reacted at room temperature with the appropriate aldehyde in ethyl alcohol and in the presence of a 50% KOH/H_2O solution, to give the desired final compounds (**1-31**, Table 1). The acetophenone intermediates were obtained by reaction of 2,4-dihydroxyacetophenone with the appropriate alkyl halide to obtain the 2-OH,4-alkoxyacetophenones (**32, 33**) and 2,4-bi-functionalyzed-acetophenones (**34-37**).

2.3. Biological and Enzymatic Assays

First, 31 chalcone-based derivatives were investigated for their antileishmanial effect on the promastigotes of *L. donovani*. Then, for 16 analogues that inhibited parasite growth at micromolar level, cytotoxicity against mammalian kidney epithelial cells and affinity for TR enzyme (SPR-based assay) were also evaluated. This allowed us to identify two promising molecules in terms of activity and selectivity that were then further investigated for their ability to inhibit promastigote

130 growth of different parasitic species, including *L.tropica*, *L.major* and L.*infantum* and to affect the
131 growth *L.donovani* amastigotes. Finally, the mechanism of TR inhibition was also studied.
132
133 *2.3.1. In vitro inhibition of Leishmania promastigote growth*
134 To assess the antileishmanial potential of the synthesized compounds, a reference strain of *L.*
135 *donovani* (MHOM/NP/02/BPK282/0cl4) was employed in two different stages of the parasitic life
136 cycle; the extracellular promastigote form is found in the sandfly vector, while intracellular
137 amastigote form is specifically found in the host cell.
138 In a first experiment, 31 chalcone-based derivatives were investigated for their antileishmanial
139 efficacy on the promastigote forms of *L. donovani* (Table 1). Amphotericin B was employed as
140 reference compound. Data were expressed as IC_{50}, i.e. the concentration of compound that is
141 required to inhibit growth by 50%.
142 Among the tested chalcones, compounds **1-16** turned out to effectively inhibit the promastigote
143 growth with micromolar potency and IC_{50}/72h values ranged from 21.5 µM (compound **12**) to 3.0
144 µM (compound **6**). Concerning analogues **17-31,** no antileishmanial effect was observed at the
145 maximal dose of 40.0 µM and were then discarded from further evaluation. Among derivatives with
146 a simple phenyl function as B-ring included in Series 1 (**7**, **19-21**), the substituent at the 2-position
147 of the A-ring markedly affected the inhibitory behaviour against *Leishmania*. In details, compound
148 **7**, bearing a methoxy function, showed an IC_{50}/72h of 15.0 µM, while the presence of hydroxy,
149 acethoxy, and prenyloxy (**19**, **20** and **21**, respectively) rendered the derivatives almost inactive. By
150 keeping the most favourable 2-methoxy-4-prenyloxy substitution pattern in the A-ring, further
151 modifications were applied to the B-aryl ring. The presence of electron-donating moieties, such as
152 methoxy groups, on several positions of the B-ring (compounds **8**, **23**, **24**) gave different results, as
153 only the bulky 3,4,5-trimethoxylated analogue **8** proved to inhibit parasite growth with an IC_{50}/72h
154 of 11.0 µM. The effect of different electron-withdrawing groups, namely bromo, nitro, and fluoro,
155 on the *para* position of the B-ring (compounds **5**, **6**, and **22**, respectively) was also investigated:

compound **6**, with the nitro substituent, resulted to be the most active among the series, showing an IC_{50}/72h of 3.0 μM, followed by the bromo-derivative **5** (IC_{50}/72h = 16.0 μM). The introduction of a heterocyclic furyl group (**18**) led to a loss of activity, while a 4- and 3-pyridyl moiety (**3** and **4**, respectively) allowed to retain good activities (IC_{50}/72h = 10.5 μM). The corresponding pyridyl-based analogues (**1** and **2**), characterized by a 2-hydroxyl function, retained leishmanicidal activity (IC_{50}/72h = 5.0 μM and 8.5 μM, respectively).

A different trend of potency was observed in the 4-propargyloxylated Series 2 upon applying different B-ring functionalization. The insertion on B-ring of methoxy groups (**27**, **28** and **29**-**31**) and *para*-NO_2 functions (analogues **25** and **26**) led to inactive compounds. Interestingly, the presence of a *para*-F phenyl B-ring and of a 2-propargyloxylated A-ring (compound **16**) conferred an effective ability to inhibit *Leishmania* growth (IC_{50}/72h = 12.5 μM). Moreover, the *para*-Br derivatives **12** and **15** retained a moderate antileishmanial activity (IC_{50}/72h = 21.5 μM and 15.0 μM, respectively) that was comparable to the corresponding Br-derivative **5** of Series 1. The pyridine-based analogues **10**, **11**, and **13**, **14** with a 2-methoxy-4-propargyloxy and 2,4-bis-propargyloxy A-ring, respectively, showed low micromolar potencies (IC_{50}/72h values ranging from 4.0 μM to 9.5 μM), similar to that of the corresponding Series 1 analogues (**1**-**4**). A reduction of activity was observed for compound **9**, designed as the 2-hydroxy congener of **11** and **14** derivatives.

Compound **6** and **16** were further investigated for their antileishmanial efficacy on the promastigote forms of three other parasitic species, ie *L. tropica*, *L. major* and *L. infantum*. Interestingly, the results obtained highlight diverse susceptibilities of different parasitic species to the compounds., In detail, compound **6** exhibited an IC_{50}/72h of 5.2 μM, 3.3 μM and 1.6 μM on*L. tropica* , *L. major* and *L. infantum*, respectively, while compound **16** showed an IC_{50}/72h of 13 μM, 10 μM and 1.6 μM on *L. tropica*, *L. major* and *L. infantum*, respectively. Thus, both compound **6** and **16** exhibited the highest inhibitory activity on *L. infantum*, revealing *L. infantum* as the most susceptible species to the examined chalcones.

2.3.2 In vitro mammalian cell toxicity

The cytotoxic effect against mammalian cells was evaluated for the most active chalcones (**1-16)** by using Vero cell line (mammalian kidney epithelial cells) (Table 1). Data were expressed as 50% cytotoxic concentration (CC_{50}). The tested compounds generally displayed moderate to low cytotoxicity, with CC_{50}/72h values above 30 µM. In particular, analogues **5**, **6** and **16** were characterized by low toxicity, with cytotoxic effect detected only at 600 µM. On the contrary, the pyridine-based chalcones showed an unfavorable SI due to their moderate cytotoxic effects. It is noteworthy that CC_{50}/72h value of the reference compound amphotericin B was 200 µM, lower than those of compound **6** and **16.** The cytotoxic effect against human acute monocytic leukemia cell line (THP-1) was also evaluated (Table 1) and the selectivity index (SI) was calculated as CC_{50}/IC_{50} ratio. Analogue **5** showed a higher cytotoxic effect on THP-1 than on the Vero cell line. On the other hand, compound **6** and **16**, the most promising of the series, showed the same low cytotoxic effect on the Vero cell line and on THP-1. The cytotoxicity assays allowed to identify compounds **6** and **16** as the most promising of the series. Indeed they showed a remarkable antileishmanial potency against the extracellular form of the parasite (IC_{50}/72h = 3.0 µM and 12.5 µM, for compound **6** and **16**, respectively) that was coupled with a good SI on mammalian cells (200 and 48, for compound **6** and **16**, respectively).

2.3.3 Inhibition of L. donovani amastigote growth

Considering the promising results obtained for **6** and **16**, these compounds were selected to be tested for their efficacy against the amastigote stage of *L. donovani*. The amastigote assay was performed by using metacyclic promastigotes to infect differentiated THP-1 macrophagic cells; amastigotes transformed from metacyclic promastigotes proliferated inside host macrophages. An inversion of potencies was observed when focusing on inhibitory activity of **6** and **16** on amastigotes growth, with respect to activities recorded on promastigotes (Figure 2a-

2b). Indeed, compound **16** exhibited a higher inhibitory effect on amastigotes than on promastigotes (4.5 μM vs 12.5 μM, IC_{50}/72h calculated on amastigote and promastigote cultures, respectively), while compound **6** showed a lower potency on amastigotes than on promastigotes (14.0 μM vs 3.0 μM, IC_{50}/72h detected on amastigote and promastigote cultures, respectively).

2.3.4. Evaluation of activity toward trypanothione reductase

2.3.4.1. Surface Plasmon Resonance screening

For Surface Plasmon Resonance (SPR) experiments, TR from *Leishmania* spp. has been immobilized by amine coupling on COOH5 sensorchips, while chalcones were analytes; FastStep SPR experiments were performed by stepped analyte gradient injections (ranging between 1.5 and 100 μM). Screening of the 16 most active chalcones (compounds **1**-**16**) demonstrated that two molecules, compounds **6** and **16**, interacted directly and with high affinity with TR. K_D values calculated for these compounds were K_D (compound **6**) = 0.6 ± 0.2 μM and K_D (compound **16**)= 2.4 ± 0.5 μM (Figure 3).

2.3.4.2. Enzymatic assays

Kinetic studies were performed on compound **6,** endowed with the highest activity against the promastigote forms of *L. donovani* and affinity toward TR. Steady state kinetic experiments were carried out at various concentrations of TS_2 and compound **6,** while fixed TR and NADPH concentrations (10 nM and 40 μM, respectively) were maintained. After starting the reaction by the addition of NADPH, the absorbance decrease at 340 nm, indicative of NADPH oxidation, was measured. As shown in Figure 4, compound **6** competitively inhibited the binding of TS_2 to TR. Each line in the Dixon plot represents linear regression analysis of reciprocal of average fitted rates of TS_2 reduction for different substrate concentrations, as a function of inhibitor concentration. The K_M and k_{cat} of TR used for the K_i calculation were 23.0 ± 1.0 μM and 11.4 ± 0.3 s^{-1} respectively

232 [17]. The value of Ki calculated from the Dixon plot analysis was 0.45 ± 0.11 μM, about three times
233 lower than that of Sb(III) (1.5 μM) [13].
234
235 *2.4. Docking studies*
236 The crystal structure of TR from *L. infantum* revealed two crucial cysteine residues (Cys52 and
237 Cys57) in the active site, involved in a concerted nucleophilic attack to the TS_2 disulfide bridge to
238 produce the reduced substrate $T(SH)_2$. In order to gain functional and structural insight into the
239 mechanism of inhibition, molecular docking simulations of compound **6** to TR were performed
240 using the x-ray structures of the enzyme in both reduced and oxidized states. Figure 5a illustrates
241 the most probable and energetically favourable binding modes of compound **6** at the active site of
242 TR in oxidized state (PDB code: 2JK6) and Figure 5b shows the conformation with the lowest
243 energy in the most populated cluster. As shown in TableS1, the most populated cluster contains
244 32/100 poses and the lowest energy pose in this cluster displays a binding energy of -7.63 kcal/mol
245 corresponding to a Ki=2.56 μM. Figure 5c displays the conformation with the lowest energy in the
246 most populated cluster, resulting from the docking procedure performed using TR in reduced state
247 (PDB code: 4ADW); the clusters and the energies of the poses are reported in TableS2. In this case,
248 the most populated cluster contains 16/100 poses and the lowest energy pose in this cluster displays
249 a binding energy of -6.66 kcal/mol, corresponding to a Ki=13.19 μM.
250 As shown in Figure 5, both the docking procedures performed using the TR structures in the
251 oxidized and reduced state gave similar results. Interestingly, in both the procedures the most
252 populated clusters occupy the same portion of the trypanothione cavity volume. Compound **6** binds
253 to TR in both oxidized and reduced states at the same hydrophobic pocket close to the two catalytic
254 cysteines lined by the following residues: Ile339, Ile458', His461', E466', E467', S470', F396',
255 L399'. Compound **6** establishes electrostatic interactions with and K61, E467' and S470'.
256 Interestingly, compound **6** appears to have a higher affinity for the oxidized form of TR.
257

3. DISCUSSION

To support the urgent need of safe and effective agents against leishmaniasis. a plethora of bioactive compounds with antileishmanial activity and acting through different mechanisms have been synthetized [27, 28]. Evidence indicates that a number of natural and synthetic chalcones exhibit antileishmanial activity [25, 29-32]. In this study, we evaluated the antileishmanial effect of a small library of synthetic chalcones and we investigated the mechanism of action of selected compounds. Among the 31 tested compounds, 16 (**1-16**) turned out to inhibit the promastigote form of *L.donovani* with micromolar potency, and among them, two (**6** and **16**) showed good potency (IC_{50}/72h values of 3.0 and 12.5 µM, respectively), even if lower with respect to the reference drug amphotericin B. Furthermore compounds **6** and **16** maintained a good inhibitory activity when tested on amastigotes of *L.donovani* (IC_{50} values of 14.0 and 4.5 µM, respectively). Interestingly, these derivatives were characterized by low toxicity when tested on Vero cells and THP-1 cells, being three times less toxic than amphotericin B and thus exhibiting a very favorable SI.

Moreover, compounds **6** and **16** efficiently inhibited the promastigote growth of other leishmanial species, including *L.tropica*, *L.major* and *L.infantum*, being particularly active on *L.infantum*.

In an effort to assess the mechanism by which **6** and **16** inhibit *Leishmania* growth, we evaluated their affinity and activity against TR, a pivotal enzyme involved in the parasite detoxification. The enzymes of the trypanothione pathway are not present in mammals, and are often considered among the most promising antileishmanial targets. However, it was previously demonstrated that at least 90% of TR inactivation needs to be obtained by inhibitor compounds to kill the parasite; therefore, effective TR inhibitors should have submicromolar inhibition activity [12]. Here, we observed that compound **6** showed a submicromolar Ki value vs. TR (0.45 ± 0.11 µM) that is about 6 times lower than the IC_{50}/72h value vs. promastigotes and 30 times lower than the IC_{50}/72h vs. the amastigotes. This result is in agreement with numerous results present in literature showing that specific and efficient trypanosomatid TR inhibitors have been found to be less active on the parasites growth. This apparent paradox was shown by Krieger and coworkers who produced conditioned TR

knockout in *T. brucei* [33], demonstrating that the redox metabolism of the parasite was affected only when TR was titrated down to less than 5% of normal. Thus, compound **6** is a good TR inhibitor, with a Ki value remarkably lower than Sb(III) and azole-based compounds and in the same order of magnitude of RDS 777, a diaryl sulphide derivative [17, 18].

The docking experiments furnished a possible binding mode of compound **6** to the catalytic site. Indeed, compound 6 binds to TR in both the oxidized and reduced states to a hydrophobic pocket close to the catalytic site, which was already shown to be part of RDS 777 binding site in the TR trypanothione cleft. Interestingly, F396' and E467' lining the compound **6** binding site have been already identified as important residues to establish interaction with other TR inhibitors [18].

This study has some limitations, including the employment of a small library of chalcones for the screening of antileishmanial activity and the lack of *in vivo* pharmacokinetic and pharmacodynamic testing of the selected compounds.

4. CONCLUSIONS

A small library of 31 chalcone-based analogues were synthetized and tested for their antileishmanial activity. Among tested compounds, **6** and **16** were found to be significantly active in *in vitro* evaluation against *L. donovani* promastigotes and amastigotes without eliciting cytotoxic effects towards human cells, thus showing optimal performance in terms of potency and selectivity. Furthermore, compounds **6** and **16** inhibited the promastigote growth of other leishmanial species, including *L. tropica*, *L. major* and *L. infantum*. Finally, compounds **6** and **16** interacted with TR and compound **6** effectively inhibited TR activity, providing evidence that TR inhibition could represent one of the possible mechanisms of action of this molecule. In conclusion, the effective inhibitory activity against different *Leishmania* species, the lack of toxicity on mammalian cells and the ability to block a crucial parasite enzyme target, highlight the potential for the chalcone **6** to be further optimized and to develop novel drug candidates against leishmaniasis.

5. EXPERIMENTAL SECTION

5.1. Chemistry.

Starting materials, unless otherwise specified, were used as high grade commercial products. Solvents were of analytical grade. Reaction progress was followed by thin layer chromatography (TLC) on precoated silica gel plates (Merck Silica Gel 60 F254) and then visualized with a UV254 lamplight. Chromatographic separations were performed on Merck silica gel columns by flash method (Kieselgel 40, 0.040-0.063 mm, 240 – 400 mesh). Melting points were determined in open glass capillaries, using a Büchi apparatus and are uncorrected. ^{1}H NMR and ^{13}C NMR spectra were recorded on a Varian Gemini spectrometer 400 MHz and 101 MHz, respectively, and chemical shifts (δ) are reported as parts per million (ppm) values relative to tetramethylsilane (TMS) as internal standard; standard abbreviations indicating spin multiplicities are given as follows: s (singlet), d (doublet), t (triplet), br (broad), q (quartet) or m (multiplet); coupling constants (*J*) are reported in Hertz (Hz). Mass spectra were recorded on a Waters ZQ 4000 apparatus operating in electrospray mode (ES). Analyses indicated by the symbols of the elements were within ± 0.4 % of the theoretical values. Compounds were named relying on the naming algorithm developed by CambridgeSoft Corporation and used in Chem-BioDraw Ultra 14.0.

5.2. Williamson Reaction: General Procedure

A mixture of selected hydroxylated acetophenone (1.0 eq), alkyl halide (1.1-1.5 eq), K_2CO_3 (1.1 eq) in acetone, was heated for 6-10 h at 80 °C; reaction progress was monitored by TLC. Upon reaction completion, the mixture was hot filtered and the solvent was evaporated under reduced pressure. The resulting crude product was purified by column chromatography over a silica gel using a mixture of petroleum ether/EtOAc as the eluent to give the desired pure product.

5.2.1. 1-(2-hydroxy-4-((3-methylbut-2-en-1-yl)oxy)phenyl)ethan-1-one (**32**) Reaction of 2,4-dihydroxyacetophenone (5.0 mmol, 0.75 g) and 3,3-dimethylallyl bromide (5.5 mmol, 0.82 g) gave the crude **32** that was purified by flash chromatography (petroleum ether/EtOAc 9:1), 97% yield, mp 42-44 °C. ^{1}H-NMR ($CDCl_3$) δ 1.88 (s, 3H, CH_3), 1.91 (s, 3H, CH_3), 2.55 (s, 3H, $COCH_3$), 4.65 (d, 2 H, *J* = 6.6 Hz, OCH_2), 5.55 (t, 1H, *J* = 6.6 Hz, CH), 6.44 (d, *J* = 1.8 Hz, 1H, H-3), 6.54 (dd, *J* = 1.8 and 8.6 Hz, 1H, H-5), 7.78 (d, *J* = 8.6 Hz, 1H, H-6).

*5.2.2. 1-(2-hydroxy-4-(prop-2-yn-1-yloxy)phenyl)-1-ethanone (**33**).* Reaction of 2,4-dihydroxyacetophenone (5.0 mmol, 0.75 g) and propargyl bromide solution 80 wt. % in toluene (5.5 mmol, 0.80 g) gave the crude final product **33** that was purified by flash chromatography (petroleum ether/EtOAc 7:3), 93% yield, mp 64-66 °C. ^{1}H-NMR ($CDCl_3$) δ 2.55 (s, 3H, CH_3), 2.60 (s, 1H, CH), 4.72 (s, 2H, OCH_2), 6.44 (d, *J* = 1.8 Hz, 1H, H-3), 6.55 (dd, *J* = 1.8 and 8.6 Hz, 1H, H-5), 7.70 (d, *J* = 8.6 Hz, 1H, H-6).

*5.2.3. 1-(2-methoxy-4-((3-methylbut-2-en-1-yl)oxy)phenyl)ethan-1-one (**34**).* Reaction of **32** (4.2 g, 20.1 mmol) with methyl iodide (4.18 g, 30.25 mmol) gave the crude final product **34** that was purified by flash chromatography (petroleum ether/EtOAc 9.75:0.25), 93% yield, mp 74-76 °C. ^{1}H-NMR ($CDCl_3$) δ 1.77 (s, 3H, CH_3), 1.81 (s, 3H, CH_3), 2.57 (s, 3H, $COCH_3$), 3.00 (s, 3H, OCH_3), 4.58 (d, 2 H, *J* = 6.6 Hz, OCH_2), 5.48 (t, 1H, *J* = 6.6 Hz, CH), 6.42 (d, *J* = 1.8 Hz, 1H, H-3), 6.53 (dd, *J* = 1.8 and 8.6 Hz, 1H, H-5), 7.83 (d, *J* = 8.6 Hz, 1H, H-6).

*5.2.4. 1-(2,4-bis((3-methylbut-2-en-1-yl)oxy)phenyl)ethan-1-one (**35**).* Reaction of **32** (4.2 g, 20.1 mmol) with 3,3-dimethylallyl bromide (4.41 g, 30.25 mmol) gave the crude final product **35** that was purified by flash chromatography (petroleum ether/EtOAc 9.75:0.25) as transparent oil, 56 % yield. ^{1}H NMR ($CDCl_3$) δ 1.75 (s, 3H, CH_3), 1.80 (s, 3H, CH_3), 1.84 (s, 3H, CH_3), 1.88 (s, 3H, CH_3), 2.55 (s, 3H, $COCH_3$), 4.50 (d, 2H, *J* = 6.6 Hz, OCH_2), 4.57 (d, 2H, *J* = 6.6 Hz, OCH_2), 5.44

(t, 1H, *J* = 6.6 Hz, CH), 5.60 (t, 1H, *J* = 6.6 Hz, CH), 6.45 (d, *J* = 1.8 Hz, 1H, H-3), 6.58 (dd, *J* = 1.8 and 8.6 Hz, 1H, H-5), 7.81 (d, *J* = 8.6 Hz, 1H, H-6).

*5.2.5. 1-(2-methoxy-4-(prop-2-yn-1-yloxy)phenyl)ethan-1-one (**36**).* Reaction of **33** (3.16 g, 17.7 mmol) with methyl iodide (3.75 g, 26.55 mmol) gave the crude final product **36** that was purified by flash chromatography (petroleum ether/EtOAc 9.5:0.5), 92%, yield, mp 93-95 °C. ^{1}H NMR ($CDCl_3$) δ 2.59-2.61 (m, 4H, $COCH_3$ and CH), 3.95 (s, 3H, OCH_3), 4.78 (s, 2H, OCH_2), 6.57 (d, *J* = 1.8 Hz, 1H, H-3), 6.59 (dd, *J* = 1.8 and 8.6 Hz, 1H, H-5), 7.82 (d, *J* = 8.6 Hz, 1H, H-6).

*5.2.6. 1-(2,4-bis(prop-2-yn-1-yloxy)phenyl)ethan-1-one (**37**).* Reaction of **33** (3.16 g, 17.7 mmol) with propargyl bromide solution 80 wt. % in toluene (4.97 g, 26.55 mmol) gave the crude final product **37** that was purified by flash chromatography (petroleum ether/EtOAc 9.5/0.5), 75 % yield, mp 101-103 °C. ^{1}H NMR ($CDCl_3$) δ 2.59-2.61 (m, 5H, $COCH_3$ and CH_2), 4.78 (s, 2H, OCH_2), 4.81 (s, 2H, OCH_2), 6.57 (d, *J* = 1.8 Hz, 1H, H-3), 6.57 (dd, *J* = 1.8 and 8.6 Hz, 1H, H-5), 7.80 (d, *J* = 8.6 Hz, 1H, H-6).

5.3. Claisen–Schmidt reaction: *General Procedure*

To an ethanol solution of acetophenone (**32-37**, 1.0 eq) and the selected benzaldehyde (1.1 eq), a KOH aqueous solution (50 % p/v, 6 eq) was added dropwise. The reaction mixture was stirred at room temperature overnight, then diluted with water and acidified with 6N HCl. The separated solid was collected by *vacuum* filtration and was purified by flash chromatography using petroleum ether/EtOAc as eluent. The final products were crystallized from suitable solvent.

*5.3.1. (E)-1-(2-hydroxy-4-((3-methylbut-2-en-1-yl)oxy)phenyl)-3-(pyridin-4-yl)prop-2-en-1-one (**1**).* Starting from **32** (0.22 g, 1.0 mmol) and 4-pyridinecarboxaldehyde (0.19 g, 1.1 mmol) the crude final product **1** was obtained and was purified by crystallization from EtOH to obtain a red-orange solid (0.14 g), 45% yield, mp 102-103 °C. ^{1}H NMR ($CDCl_3$) δ 1.77 (s, 3H, CH_3), 1.82 (s, 3H, CH_3), 4.59 (d, *J* = 6.4 Hz, 2H, OCH_2), 5.49-5.53 (m, 1H, CH=C), 6.50 (d, *J* = 1.8 Hz, 1H, H-3), 6.52 (dd,

381 *J* = 1.8 and *J*= 8.4 Hz, 1H, H-5), 7.49 (d, *J* = 4.4 Hz, 2H, H-2' and H-6'), 7.71 (d, *J* = 15.6 Hz, 1H,
382 =CH), 7.73 (d, *J* = 15.6 Hz, 1H, CH=), 7.81 (d, *J* = 8.8 Hz, 1H, H-6), 8.70 (d, *J* = 4.4 Hz, 2H, H-3'
383 and H-5'). ^{13}C NMR ($CDCl_3$) δ 18.2, 25.7, 65.3, 101.7, 108.6, 113.8, 118.5, 122.0, 124.7, 131.2,
384 138.5, 141.0, 142.0, 148.8, 149.5, 166.0, 166.9, 192.1. ESI-MS (*m/z*): 310 (M + H); Anal.
385 $C_{19}H_{19}NO_3$ (C, H, N).

386 *5.3.2. (E)-1-(2-hydroxy-4-((3-methylbut-2-en-1-yl)oxy)phenyl)-3-(pyridin-3-yl)prop-2-en-1-one (**2**).*
387 Starting from **32** (0.22 g, 1.0 mmol) and 3-pyridinecarboxaldehyde (0.19 g, 1.1 mmol) gave the
388 crude final product **2** that was purified by crystallization from EtOH to obtain a orange solid (0.21
389 g), 67% yield, mp 108-109 °C. ^{1}H NMR ($CDCl_3$) δ 1.77 (s, 3H, CH_3), 1.82 (s, 3H, CH_3), 4.59 (d, *J*
390 = 6.4 Hz, 2H, OCH_2), 5.49-5.53 (m, 1H, CH=C), 6.51 (d, *J* = 2.0 Hz 1H, H-3), 6.53 (dd, *J* = 8.8 and
391 2.0 Hz, 1H, H-5), 7.32-7.36 (m, 1H, H-5'), 7.62 (d, *J* = 15.6 Hz, 1H,=CH), 7.82 (d, *J* = 16.0 Hz, 1H,
392 CH=), 7.84 (d, *J* = 8.8 Hz, 1H, H-6'), 7.79 (d, *J* = 7.6 Hz, 1H, H-6), 8.61 (d, *J* = 4.8 Hz, 1H, H-4'),
393 8.94 (s, 1H, H-2'). ^{13}C NMR ($CDCl_3$) δ 18.66, 25.6, 65.2, 102.7, 107.6, 113.8, 119.2, 123.5, 125.7,
394 131.2, 138.4, 144.0, 144.1, 149.8, 149.5, 166.0, 166.7, 192.8. ESI-MS (*m/z*): 310 (M + H); Anal.
395 $C_{19}H_{19}NO_3$ (C, H, N).

396 *5.3.3. (E)-1-(2-methoxy-4-((3-methylbut-2-en-1-yl)oxy)phenyl)-3-(pyridin-4-yl)prop-2-en-1-one (**3**).*
397 Starting from **34** (0.23 g, 1.0 mmol) and 4-pyridinecarboxaldehyde (0.19 g, 1.1 mmol) gave the
398 crude final product **3** that was purified by flash chromatography (DCM/MeOH 9.75:0.25) and then
399 crystallized from AcOEt/n-hexane to obtain a solid(0.09 g), 30% yield, mp 102-103 °C. ^{1}H NMR
400 ($CDCl_3$) δ 1.79 (s, 3H, CH_3), 1.82 (s, 3H, CH_3), 3.96 (s, 3H, OCH_3), 4.51 (d, *J* = 6.4 Hz, 2H,
401 OCH_2), 5.44-5.51 (m, 1H, CH=C), 6.30 (d, *J* = 1.8 Hz, 1H, H-3), 6.42 (dd, *J* = 1.8 and 8.4 Hz, 1H,
402 H-5), 7.49 (d, *J* = 4.4 Hz, 2H, H-2' and H-6'), 7.70 (d, *J* = 15.6 Hz, 1H, =CH), 7.72 (d, *J* = 15.6 Hz,
403 1H, CH=), 7.80 (d, *J* = 8.8 Hz, 1H, H-6), 8.65 (d, *J* = 4.4 Hz, 2H, H-3' and H-5'). ^{13}C NMR
404 ($CDCl_3$) δ 18.5, 24.5, 55.2, 64.3, 101.9, 107.6, 113.8, 119.1, 123.0, 125.7, 131.2, 138.5, 144.1,
405 144.6, 148.8, 149.3, 162.1, 166.5, 192.5. ESI-MS (*m/z*): 324 (M + H); Anal. $C_{20}H_{21}NO_3$ (C, H, N).

406 *5.3.4. (E)-1-(2-methoxy-4-((3-methylbut-2-en-1-yl)oxy)phenyl)-3-(pyridin-3-yl)prop-2-en-1-one (**4**).*
407 Starting from **34** (0.23 g, 1.0 mmol) and 3-pyridinecarboxaldehyde (0.19 g, 1.1 mmol) gave the
408 crude final product **4** that was purified by flash chromatography (DCM/MeOH 9.75:0.25) and then
409 crystallized from AcOEt/n-hexane to obtain an orange solid (0.14 g), 45% yield, mp 98-100 °C. ^{1}H
410 NMR ($CDCl_3$) δ 1.78 (s, 3H, CH_3), 1.83 (s, 3H, CH_3), 3.93 (s, 3H, OCH_3), 4.78 (d, *J* = 4 Hz, 2H,
411 OCH_2) 5.49-5.53 (m, 1H, CH=C), 6.61 (s, 1H, H-3), 6.66 (d, *J* = 8.8 Hz, 1H, H-5) 7.34-7.37 (m,
412 1H, H-5'), 7.56 (d, *J* = 15.6 Hz, 1H,=CH), 7.62 (d, *J* = 16 Hz, 1H, CH=), 7.80 (d, *J* = 8.8 Hz, 1H,
413 H-6'), 7.89 (d, *J* = 7.6 Hz, 1H, H-6), 8.60 (d, *J* = 4.8 Hz, 1H, H-4'), 8.84 (s, 1H, H-2'). ^{13}C NMR
414 ($CDCl_3$) δ 18.4, 24.7, 55.8, 64.9, 101.5, 107.6, 119.3, 123.5, 127.1, 129.7, 131.3, 132.7, 138.4,
415 141.1, 148.0, 148.6, 149.3, 163.3, 168.3, 192.2. ESI-MS (*m/z*): 324 (M + H); Anal. $C_{20}H_{21}NO_3$ (C,
416 H, N).

417 *5.3.5. (E)-3-(4-bromophenyl)-1-(2-methoxy-4-((3-methylbut-2-en-1-yl)oxy)phenyl)prop-2-en-1-one*
418 *(**5**).* Starting from **34** (0.23 g, 1.0 mmol) and 4-bromobenzaldehyde (0.20 g, 1.1 mmol) gave the
419 crude final product **5** that was purified by flash chromatography (petroleum ether/AcOEt 4:1) and
420 then crystallized from AcOEt/n-hexane to obtain a yellow solid (0.32 g), 81% yield, mp 96-98 °C.
421 ^{1}H NMR ($CDCl_3$) δ 1.78 (s, 3H, CH_3), 1.83 (s, 3H, CH_3), 3.91 (s, 3H, OCH_3), 4.59 (d, *J* = 6.4 Hz,
422 2H, OCH_2), 5.49-5.53 (m, 1H, CH=C), 6.64 (d, *J* = 2.0 Hz, 1H, H-3), 6.72 (dd, *J* = 2.0 and 8.8 Hz,
423 1H, H-5), 7.62 (d, *J* = 15.6 Hz, 1H, =CH), 7.66 (d, *J* = 15.8 Hz, 1H, CH=), 7.76 (d, *J* = 8.8 Hz, 2H,
424 H-2' and H-6'), 7.80 (d, *J* = 8.4 Hz, 1H, H-6), 8.24 (d, *J* = 8.8 Hz, 2H, H-3' and H-5'). ^{13}C NMR
425 ($CDCl_3$) δ 18.3, 24.9, 54.2, 65.1, 100.3, 106.6, 118.7, 119.9, 123.4, 128.2, 128.4, 131.8, 133.5,
426 138.9, 145.4, 162.4, 168.8, 191.2. ESI-MS (*m/z*): 402 (M + H); Anal. $C_{21}H_{21}BrO_3$ (C, H,).

427 *5.3.6. (E)-1-(2-methoxy-4-((3-methylbut-2-en-1-yl)oxy)phenyl)-3-(4-nitrophenyl)prop-2-en-1-one*
428 *(**6**).* Starting from **34** (0.23 g, 1.0 mmol) and 4-nitrobenzaldehyde (0.17 g, 1.1 mmol) gave the crude
429 final product **6** that was purified by crystallization from EtOH to obtain a yellow solid (0.28 g),
430 77% yield, mp 147-147 °C. ^{1}H NMR ($CDCl_3$) δ 1.77 (s, 3H, CH_3), 1.82 (s, 3H, CH_3), 3.93 (s, 3H,

OCH_3), 4.57 (d, *J* = 6.4 Hz, 2H, OCH_2), 5.49-5.53 (m, 1H, CH=C), 6.52 (d, *J* = 1.6 Hz, 1H, H-3), 6.58 (dd, *J* = 1.6 and 8.0 Hz, 1H, H-5), 7.68 (d, *J* = 16.0 Hz, 1H, =CH), 7.59 (d, *J* = 16.0 Hz, 1H, CH=), 7.72 (d, *J* = 8.4 Hz, 1H, H-2' and H-6'), 7.81 (d, *J* = 8.4 Hz, 1H, H-6), 8.26 (d, *J* = 8.4 Hz, 1H, H-3' and H-5'). ^{13}C NMR ($CDCl_3$) δ 18.2, 25.8, 55.7, 65.1, 105.8, 118.9, 121.3, 124.1, 128.6, 131.0, 133.2, 138.2, 141.9, 160.7, 164.2, 183.2. ESI-MS (*m/z*): 368 (M + H); Anal. $C_{21}H_{21}NO_5$ (C, H, N).

*5.3.7. (E)-1-(2-methoxy-4-((3-methylbut-2-en-1-yl)oxy)phenyl)-3-phenylprop-2-en-1-one (**7**).* Starting from **34** (0.23 g, 1.0 mmol) and benzaldehyde (0.11 g, 1.1 mmol) gave the crude final product **7** that was purified by flash chromatography (petroleum ether/AcOEt 9.5:0.5) to obtain a yellow solid (0.14 g), 42% yield, mp 147-149 °C. ^{1}H NMR ($CDCl_3$) δ 1.78 (s, 3H, CH_3), 1.82 (s, 3H, CH_3), 3.90 (s, 3H, OCH_3), 4.58 (d, *J* = 6.4 Hz, 2H, OCH_2), 5.49-5.53 (m, 1H, CH=C), 6.53 (d, *J* = 1.6 Hz, 1H, H-3), 6.57 (dd, *J* = 1.6 and 8.0 Hz, 1H, H-5), 7.30-7.43 (m, 3H, H-3'-H-5'), 7.53 (d, *J* = 15.6 Hz, 1H, CH=), 7.61-7.67 (m, 2H, H-2' and H-6'), 7.68 (d, *J* = 15.6 Hz, 1H, CH=), 7.77 (d, *J* = 8.4 Hz, 1H, H-6). ^{13}C NMR ($CDCl_3$) δ 18.2, 25.8, 55.7, 65.0, 99.3, 105.8, 118.9, 122.0, 127.2, 128.2, 128.8, 129.9, 132.8, 135.5, 141.9, 160.4, 163.5, 190.6. ESI-MS (*m/z*): 323 (M + H); Anal. $C_{20}H_{22}O_3$ (C, H).

*5.3.8. (E)-1-(2-methoxy-4-((3-methylbut-2-en-1-yl)oxy)phenyl)-3-(3,4,5-trimethoxyphenyl)prop-2-en-1-one (**8**).* Starting from **34** (0.23 g, 1.0 mmol) and 3,4,5-trimethoxybenzaldehyde (0.21 g, 1.1 mmol) gave the crude final product **8** that was purified by crystallization from EtOH to obtain a yellow solid (0.29 g), 71% yield, mp 62-64 °C. ^{1}H NMR ($CDCl_3$) δ 1.78 (s, 3H, CH_3), 1.82 (s, 3H, CH_3), 3.90 (s, 3H, OCH_3), 3.89 (s, 9H, OCH_3), 4.57 (d, *J* = 6.4 Hz, 2H, OCH_2), 5.49-5.53 (m, 1H, CH), 6.52 (d, *J* = 1.6 Hz, 1H, H-3), 6.57 (dd, *J* = 1.6 and 8.0 Hz, 1H, H-5), 6.81 (s, 2H, H-2' and H-6'), 7.34 (d, *J* = 15.6 Hz, 1H, CH=), 7.54 (d, *J* = 15.6 Hz, 1H, CH=), 7.70 (d, *J* = 8.4 Hz, 1H, H-6). ^{13}C NMR ($CDCl_3$) δ 18.7, 25.7, 55.6, 56.7, 56.9, 60.5, 63.8, 99.9, 103.8, 107.4, 118.5, 118.9, 123.0,

126.6, 131.3, 132.8, 138.5, 138.7, 145.9, 153.1, 153.8, 162.2, 168.8, 190.6. ESI-MS (*m/z*): 413 (M + H); Anal. $C_{24}H_{28}O_6$ (C, H).

*5.3.9. (E)-1-(2-hydroxy-4-(prop-2-yn-1-yloxy)phenyl)-3-(pyridin-3-yl)prop-2-en-1-one (**9**).* Starting from **33** (0.19 g, 1.0 mmol) and 3-pyridinecarboxaldehyde (0.19 g, 1.1 mmol) gave the crude final product **9** that was purified by crystallization from EtOH to obtain an orange solid (0.22 g), 79% yield, mp 122-124 °C. ^{1}H NMR ($CDCl_3$) δ 2.58 (s, 1H, C≡CH), 4.77 (d, *J* = 1.6 Hz, 2H, OCH_2), 6.61 (d, *J* = 1.8 Hz, 1H, H-3), 6.66 (dd, *J* = 8.8 and 1.8 Hz, 1H, H-5), 7.34-7.37 (m, 1H, H-5'), 7.56 (d, *J* = 15.6 Hz, 1H, =CH), 7.64 (d, *J* = 15.6 Hz, 1H, CH=), 7.81 (d, *J* = 8.4 Hz, 1H, H-6'), 7.89 (d, *J* = 4.8 Hz, 1H, H-6), 8.60 (d, *J* = 4.8 Hz, 1H, H-4'), 8.84 (s, 1H, H-2'). ^{13}C NMR ($CDCl_3$) δ 55.8, 76.3, 76.8, 101.6, 106.7, 127.6, 129.6, 131.3, 132.6, 133.8, 134.9, 145.6, 147.9, 149.8, 160.3, 162.4, 190.1. ESI-MS (*m/z*): 280 (M + H); Anal. $C_{17}H_{13}NO_3$ (C, H, N).

*5.3.10. (E)-1-(2-methoxy-4-(prop-2-yn-1-yloxy)phenyl)-3-(pyridin-4-yl)prop-2-en-1-one (**10**).* Starting from **36** (0.20 g, 1.0 mmol) and 4-pyridinecarboxaldehyde (0.19 g, 1.1 mmol) gave the crude final product **10** that was purified by flash chromatography (DCM/MeOH 9.75:0.25) and then crystallized from ethanol to obtain a brown solid (0.11 g), 36% yield, mp 98-100 °C. ^{1}H NMR ($CDCl_3$): δ 2.56 (s, 1H, C≡CH), 3.91 (s, 3H, OCH_3), 4.75 (d, *J* = 2.0 Hz, 2H, OCH_2), 6.58 (d, *J* = 1.6 Hz, 1H, H-3), 6.64 (dd, *J* = 2 and 8.4 Hz, 1H, H-5), 7.40 (d, *J* = 5.6 Hz, 2H, H-2' and H-6'), 7.54 (d, *J* = 16.0 Hz, 1H, =CH), 7.65 (d, *J* = 16.0 Hz, 1H, CH=), 7.79 (d, *J* = 8.4 Hz, 1H, H-6), 8.63 (d, *J* = 5.6 Hz, 2H, H-3' and H-5'). ^{13}C NMR ($CDCl_3$) δ 55.7, 56.6, 76.3, 77.7, 102.5, 107.7, 113.8, 118.2, 123.5, 125.7, 130.2, 138.7, 144.5, 146.3, 149.9, 150.5, 166.0, 166.7, 192.6. ESI-MS (*m/z*): 294 (M + H); Anal. $C_{18}H_{15}NO_3$ (C, H, N).

*5.3.11. (E)-1-(2-methoxy-4-(prop-2-yn-1-yloxy)phenyl)-3-(pyridin-3-yl)prop-2-en-1-one (**11**).* Starting from **36** (0.20 g, 1.0 mmol) and 3-pyridinecarboxaldehyde (0.19 g, 1.1 mmol) gave the crude final product **11** that was purified by flash chromatography (DCM/MeOH 9.75:0.25) and then

crystallized from ethanol to obtain a yellow solid (0.21 g), 72% yield, mp 120-122 °C. ^{1}H NMR ($CDCl_3$): δ 2.58 (s, 1H, C≡CH), 3.93 (s, 3H, OCH_3), 4.78 (d, *J* = 1.6 Hz, 2H, OCH_2), 6.62 (s, 1H, H-3), 6.66 (d, *J* = 8.8 Hz, 1H, H-5), 7.32-7.36 (m, 1H, H-5'), 7.56 (d, *J* = 15.6 Hz, 1H, =CH), 7.62 (d, *J* = 16 Hz, 1H, CH=), 7.81 (d, *J* = 8.8 Hz, 1H, H-6'), 7.89 (d, *J* = 8 Hz, 1H, H-6), 8.61 (d, *J* = 4.4 Hz, 1H, H-4'), 8.84 (s, 1H, H-2'). ^{13}C NMR ($CDCl_3$) δ 55.7, 56.6, 76.3, 77.7, 101.7, 108.5, 113.3, 122.3, 125.7, 131.2, 136.5, 141.0, 142.0, 148.8, 149.5, 151.2, 166.5, 166.9, 192.0. ESI-MS (*m/z*): 294 (M + H); Anal. $C_{18}H_{15}NO_3$ (C, H, N).

5.3.12. (E)-3-(4-bromophenyl)-1-(2-methoxy-4-(prop-2-yn-1-yloxy)phenyl)prop-2-en-1-one ***(12)****.* Starting from **36** (0.20 g, 1.0 mmol) and 4-bromobenzaldheyde (0.20 g, 1.1 mmol) gave the crude final product **12** that was purified by flash chromatography (petroleum ether/EtOAc 9:1) and then crystallized from ethanol to obtain a yellow solid (0.35 g), 95% yield, mp 131-133 °C. ^{1}H NMR ($CDCl_3$) δ 2.59 (t, *J* = 2.4 Hz, 1H, C≡CH), 3.92 (s, 3H, OCH_3), 4.77 (d, *J* = 1.6 Hz, 2H, OCH_2), 6.61 (s, 1H, H-3), 6.65 (d, *J* = 8.4 Hz, 1H, H-5), 7.49 (d, *J* = 17.2 Hz, 1H, =CH), 7.53 (d, *J* = 8.4 Hz, 2H, H-2' and H-6') 7.61 (d, *J* = 15.6 Hz, 1H, CH=), 7.77 (d, *J* = 8.4 Hz, 1H, H-6) 8.26 (d, *J* = 8.8 Hz, 2H, H-3' and H-5'). ^{13}C NMR ($CDCl_3$) δ 55.9, 56.6, 76.2, 77.9, 99.7, 106.2, 122.3, 124.9, 127.1, 129.6, 130.0, 132.1, 132.0, 134.9, 140.6, 160.8, 162.0, 190.2. ESI-MS (*m/z*): 372 (M + H); Anal. $C_{19}H_{15}BrO_3$ (C, H).

5.3.13. (E)-1-(2,4-bis(prop-2-yn-1-yloxy)phenyl)-3-(pyridin-4-yl)prop-2-en-1-one ***(13)****.* Starting from **37** (0.23 g, 1.0 mmol) and 4-pyridinecarboxaldehyde (0.19 g, 1.1 mmol) gave the crude final product **13** that was purified by crystallization from EtOH to obtain a yellow solid (0.08 g), 27% yield, mp 156-158 °C. ^{1}H NMR ($CDCl_3$) δ 2.58-2.60 (m, 2H, C≡CH), 4.78 (d, *J* = 2.0 Hz, 2H, OCH_2) 4.80 (d, *J* = 2.4 Hz, 2H, OCH_2), 6.69 (d, *J* = 1.6 Hz, 1H, H-3), 6.72 (dd, *J* = 2.0 and 8.4 Hz, 1H, H-5), 7.46 (d, *J* = 5.2 Hz, 2H, H-2' and H-6'), 7.57 (d, *J* = 15.6 Hz, 1H, =CH), 7.73 (d, *J* = 15.6 Hz, 1H, CH=), 7.84 (d, *J* = 8.8 Hz, 1H, H-6), 8.66 (d, *J* = 4.4 Hz, 2H, H-3' and H-5'). ^{13}C NMR

503 ($CDCl_3$) δ 55.9, 56.0, 76.2, 77.9, 100.7, 107.6, 113.8, 118.4, 122.4, 124.7, 131.2, 138.5, 140.9,
504 142.0, 150.5, 166.7, 167.9, 192.1. ESI-MS (*m/z*): 318 (M + H); Anal. $C_{20}H_{15}NO_3$ (C, H, N).

505 *5.3.14. (E)-1-(2,4-bis(prop-2-yn-1-yloxy)phenyl)-3-(pyridin-3-yl)prop-2-en-1-one (**14**).* Starting
506 from **37** (0.23 g, 1.0 mmol) and 3-pyridinecarboxaldehyde (0.19 g, 1.1 mmol) gave the crude final
507 product **14** that was purified by crystallization from ethanol to obtain a yellow solid (0.23 g), 72%
508 yield, mp 156-158 °C. ^{1}H NMR ($CDCl_3$): δ 2.58-2.60 (m, 2H, C≡CH), 4.78 (d, *J* = 2.0 Hz, 2H,
509 OCH_2), 4.80 (d, *J* = 2.4 Hz, 2H, OCH_2), 6.51 (s, 1H, H-3), 6.53 (d, *J* = 8.8 Hz, 1H, H-5), 7.32-7.36
510 (m, 1H, H-5'), 7.62 (d, *J* = 15.6 Hz, 1H, =CH), 7.82 (d, *J* = 16 Hz, 1H, CH=), 7.84 (d, *J* = 8.8 Hz,
511 1H, H-6'), 7.79 (d, *J* = 7.6 Hz, 1H, H-6), 8.61 (d, *J* = 4.8 Hz, 1H, H-4'), 8.94 (s, 1H, H-2'). ^{13}C
512 NMR ($CDCl_3$) δ 56.3, 56.9, 76.4, 76.7, 77.9, 101.1, 107.2, 123.4, 127.6, 128.5, 130.5, 131.6, 131.7,
513 132.9, 141.0, 158.0, 159.2, 160.7, 165.0, 190.0. ESI-MS (*m/z*):318 (M + H); Anal. $C_{20}H_{15}NO_3$ (C,
514 H, N).

515 *5.3.15. (E)-1-(2,4-bis(prop-2-yn-1-yloxy)phenyl)-3-(4-bromophenyl)prop-2-en-1-one* (**15**)
516 Starting from **37** (0.23 g, 1.0 mmol) and 4-bromobenzaldheyde (0.20 g, 1.1 mmol) gave the crude
517 final product **15** that was purified by flash chromatography (petroleum ether/EtOAc 9:1) and then
518 crystallized from EtOH to obtain a yellow solid (0.37 g), 95% yield, mp 123-125 °C. ^{1}H-NMR
519 ($CDCl_3$) δ 2.57-2.59 (m, 2H, 2 C≡CH), 4.78 (d, *J* = 8.8 Hz, 4H, 2 OCH_2), 6.70 (s, 1H, H-3), 6.73 (d,
520 *J* = 8.4 Hz, 1H, H-5), 7.46-7.54 (m, 4H, H-2'-H-6'), 7.56 (d, *J* = 15.6 Hz, 1H,=CH), 7.62 (d, *J* = 16
521 Hz, 1H, CH=), 7.80 (d, *J* = 8.4 Hz, 1H, H-6). ^{13}C NMR ($CDCl_3$) δ 55.8, 56.0, 76.1, 76.3, 99.6,
522 106.1, 122.8, 124.2, 127.6, 129.6, 131.0, 132.1, 132.8, 134.9, 140.6, 160.3, 162.1, 190.1. ESI-MS
523 (*m/z*): 396 (M + H); Anal. $C_{21}H_{15}BrO_3$ (C, H).

524 *5.3.16. (E)-1-(2,4-bis(prop-2-yn-1-yloxy)phenyl)-3-(4-fluorophenyl)prop-2-en-1-one (**16**).* Starting
525 from **37** (0.23 g, 1.0 mmol) and 4-fluorobenzaldheyde (0.14 g, 1.1 mmol) gave the crude final
526 product **16** that was purified by flash chromatography (petroleum ether/EtOAc 4:1) and then

crystallized from EtOH to obtain a yellow solid (0.30 g), 91% yield, mp 159-161 °C. ^{1}H NMR ($CDCl_3$) δ 2.57-2.59 (m, 2H, 2 C≡CH), 4.77 (d, *J* = 2.4 Hz, 2H, OCH_2), 4.79 (d. *J* = 2.4 Hz, 2H, OCH_2) 6.71 (s, 1H, H-3), 6.72 (d, *J* = 2.4 Hz, 1H, H-5), 7.06-7.11 (m, 2H, H-2' and H-6'), 7.48 (d, *J* = 15.6 Hz, 1H, =CH), 7.59-7.62 (m, 2H, H-3' and H-5'), 7.65 (d, *J* = 16 Hz, 1H, CH=), 7.79 (d, *J* = 9.6 Hz, 1H, H-6). ^{13}C NMR ($CDCl_3$) δ 56.0, 56.6, 76.2, 76.3, 77.7, 77.8, 101.1, 107.2, 115.8 (d, *J* = 22 Hz), 123.4, 126.8, 126.9, 130.1 (d, *J* = 8.5 Hz), 131.6, 131.7, 132.9, 141.0, 158.1, 161.7, 165.0, 190.0. ESI-MS (*m/z*): 335 (M + H); Anal. $C_{21}H_{15}FO_3$ (C, H, N).

*5.3.17. (E)-N-(4-(3-(2-methoxy-4-((3-methylbut-2-en-1-yl)oxy)phenyl)-3-oxoprop-1-en-1-yl)phenyl)acetamide (**17**).* Starting from **34** (0.23 g, 1.0 mmol) and 4-acetamidobenzaldehyde (0.18 g, 1.1 mmol) gave the crude final product **17** that was purified by crystallization from EtOH to obtain a yellow solid (0.12 g), 58% yield, mp 131-133 °C. ^{1}H NMR ($CDCl_3$) δ 1.78 (s, 3H, CH_3), 1.82 (s, 3H, CH_3), 2.21 (s, 3H, $COCH_3$), 3.90 (s, 3H, OCH_3), 4.57 (d, *J* = 6.4 Hz, 2H, OCH_2), 5.49-5.54 (m, 1H, CH), 6.52 (d, *J* = 2.0 Hz, 1H, H-3), 6.57 (dd, *J* = 8.0 and 2.0 Hz, 1H, H-5), 7.23 (br, 1H, NH), 7.46 (d, *J* = 16.0 Hz, 1H, =CH), 7.53 (d, *J* = 8.0 Hz, 2H, H-2' and H-6'), 7.57 (d, *J* = 8.0 Hz, 2H, H-3' and H-5'), 7.64 (d, *J* = 16.0 Hz, 1H, CH=), 7.75 (d, *J* = 8.2 Hz, 1H, H-6). ^{13}C NMR ($CDCl_3$) δ 18.2, 23.3, 25.8, 55.7, 65.1, 105.8, 118.9, 121.3, 124.5, 129.6, 131.0, 134.2, 138.6, 145.9, 161.5, 163.2, 169.9, 188.2. ESI-MS (*m/z*): 380 (M + H); Anal. $C_{19}H_{20}O_4$ (C, H).

*5.3.18. (E)-3-(furan-2-yl)-1-(2-methoxy-4-((3-methylbut-2-en-1-yl)oxy)phenyl)prop-2-en-1-one (**18**).* Starting from **34** (0.23 g, 1.0 mmol) and 2-furaldehyde (0.11 g, 1.1 mmol) gave the crude final product **18** that was purified by purified by flash chromatography (petroleum ether/EtOAc 4:1) to obtain a brown oil (0.16 g), 51% yield. ^{1}H NMR ($CDCl_3$) δ 1.77 (s, 3H, CH_3), 1.82 (s, 3H, CH_3), 3.90 (s, 3H, OCH_3), 4.58 (d, *J* = 6.4 Hz, 2H, OCH_2), 5.47-5.50 (m, 1H, CH), 6.48-6.51(m, 2H, furfuryl), 6.56 (d, *J* = 1.8 Hz, 1H, H-3), 6.64 (dd, *J* = 1.8 and 8.4 Hz, 1H, H-5), 7.26-7.27 (m, 1H, furfuryl), 7.42 (d, *J* = 15.6 Hz, 1H, =CH), 7.48 (d, *J* = 15.6 Hz, 1H, CH=), 7.76 (d, *J* = 8.2 Hz, 1H, H-6). ^{13}C NMR ($CDCl_3$) δ 18.2, 24.3, 55.7, 64.2, 101.2, 107.9, 112.5, 113.9, 119.5, 120.8, 123.4,

131.6, 138.9, 143.2, 152.5, 163.4, 168.8, 191.5. ESI-MS (*m/z*): 313 (M + H); Anal. $C_{20}H_{15}NO_3$ (C, H, N).

*5.3.19. (E)-1-(2-hydroxy-4-((3-methylbut-2-en-1-yl)oxy)phenyl)-3-phenylprop-2-en-1-one (**19**)* [34]. Reaction of **32** (1.0 mmol, 0.17 g) and benzaldehyde (1.1 mmol, 0.12 g) gave the crude **19** that was purified by crystallization from EtOH to obtain a yellow solid (0.2 g), 64% yield, mp 92-95 °C. ^{1}H NMR ($CDCl_3$) δ 1.76 (s, 3H, CH_3), 1.81 (s, 3H, CH_3), 4.56 (d, *J* = 6.0 Hz, 2H, OCH_2), 5.47 (t, *J* = 6.0 Hz, 1H, CH), 6.49 (dd, *J* = 2.0 and 8.4 Hz, 1H, H-5), 6.52 (d, *J* = 1.8 Hz, 1H, H-3), 7.43-7.55 (m, 3H, H-3'-H-5'), 7.60 (d, *J* = 15.6 Hz, 1H, =CH), 7.63-7.65 (m, 2H, H-2'and H-6'), 7.82 (d, *J* = 8.4 Hz, 1H, H-6), 7.89 (d, *J* = 15.3 Hz, 1H, CH=), 10.45 (br, 1H, OH). ^{13}C NMR ($CDCl_3$) δ 18.6, 19.5, 65.0, 101.8, 108.2, 113.9, 118.6, 120.5, 128.4, 128.8, 130.7, 130.5, 130.0, 134.2, 138.6, 143.7, 165.0, 166.1, 191.7, (In accordance with previously published spectroscopic data). MS (ESI^+) *m/z*: 309 (M + H); Anal. $C_{20}H_{20}O_3$ (C, H).

*5.3.20. (E)-1-(2,4-bis((3-methylbut-2-en-1-yl)oxy)phenyl)-3-phenylprop-2-en-1-one (**21**).* Reaction of **35** (1.0 mmol, 0.29 g) and benzaldehyde (1.1 mmol, 0.12 g) gave the crude **21** that was purified by flash chromatography (petroleum ether/EtOAc 9.75:0.25) to obtain a white oil (0.04 g), 10% yield. ^{1}H NMR ($CDCl_3$) δ 1.76 (s, 3H, CH_3), 1.82 (s, 3H, CH_3), 1.85 (s, 3H, CH_3), 1.89 (s, 3H, CH_3), 4.51 (d, *J* = 6.0 Hz, 2H, OCH_2), 4.58 (d, *J* = 6.0 Hz, 2H, OCH_2), 5.47-5.61 (m, 2H, CH), 6.47 (d, *J* = 2.0, 1H, H-3), 6.61 (dd, *J* = 2.0 and 8.4 Hz, 1H, H-5), 7.38-7.42 (m, 3H, H-3'-H-5'), 7.63-7.67 (m, 2H, H-2'and H-6'), 7.69 (d, *J* = 15.6 Hz, 1H, =C), 7.70 (d, *J* = 8.4 Hz, 1H, H-6), 7.81 (d, *J* = 15.3 Hz, 1H, C=). ^{13}C NMR ($CDCl_3$) δ 18.6, 18.7, 20.5, 20.7, 24.5, 24.8, 65.1, 65.4, 101.8, 107.3, 118.6, 119.6, 123.5, 128.1, 128.4, 128.6, 135.5, 138.0, 145.2, 162.4, 168.7, 191.9. ESI-MS (*m/z*): 378 (M + H); Anal. $C_{25}H_{28}O_3$ (C, H).

*5.3.21. (E)-3-(4-fluorophenyl)-1-(2-methoxy-4-((3-methylbut-2-en-1-yl)oxy)phenyl)prop-2-en-1-one (**22**).* Starting from **34** (0.23 g, 1.0 mmol) and 4-fluorobenzaldheyde (0.14 g, 1.1 mmol) gave the crude final product **22** that was purified by flash chromatography (petroleum ether/EtOAc 9:1) and

then crystallized from EtOH to obtain a white solid (0.12 g), 35% yield, mp 81-83 °C. ^{1}H NMR ($CDCl_3$) δ 1.78 (s, 3H, CH_3), 1.83 (s, 3H, CH_3), 3.91 (s, 3H, OCH_3), 4.59 (d, *J* =6.4 Hz, 2H, OCH_2), 5.49-5.53 (m, 1H, CH), 6.53 (d, *J* = 1.6 Hz, 1H, H-3), 6.58 (dd, *J* = 1.6 Hz and 8.0 Hz, 1H, H-5), 7.06-7.11 (m, 2H, H-2' and H-6'), 7.46 (d, *J* = 16.0 Hz, 1H, =CH), 7.57-7.60 (m, 2H, H-3' and H-5'), 7.65 (d, *J* = 16.0 Hz, 1H, CH=), 7.76 (d, *J* = 8.8 Hz, 1H, H-6). ^{13}C NMR ($CDCl_3$) δ 18.2, 25.8, 55.7, 65.1, 103.8, 107.4, 118.9, 119.3 (d, *J* = 22 Hz), 124.6, 130.0 (d, *J* = 8.5 Hz), 131.2, 138.4, 145.9, 162.7, 168.2, 193.4. ESI-MS (*m/z*): 341 (M + H); Anal. $C_{21}H_{21}FO_3$ (C, H).

*5.3.22. (E)-1-(2-methoxy-4-((3-methylbut-2-en-1-yl)oxy)phenyl)-3-(4-methoxyphenyl)prop-2-en-1-one (**23**).* Starting from **34** (0.23 g, 1.0 mmol) 4-methoxybenzaldheyde (0.14 g, 1.1 mmol) gave the crude final product **23** that was purified by flash chromatography (petroleum ether/EtOAc 4:1) and then crystallized from EtOH to obtain a yellow solid (0.23 g), 66% yield, mp 62-64 °C. ^{1}H NMR ($CDCl_3$) δ 1.78 (s, 3H, CH_3), 1.83 (s, 3H, CH_3), 3.86 (s, 3H, OCH_3), 3.90 (s, 3H, OCH_3), 4.58 (d, *J* = 7.2 Hz, 2H, OCH_2), 5.49-5.53 (m, 1H, CH), 6.53 (d, *J* = 2.0 Hz, 1H, H-3), 6.57 (dd, *J* = 2.0 Hz and 8.8 Hz, 1H, H-5), 6.90-6.95 (m, 2H, H-3' and H-5'), 7.40 (d, *J* = 16.0 Hz, 1H, =CH), 7.54-7.57 (m, 2H, H-2' and H-6'), 7.66 (d, *J* = 15.6 Hz, 1H, CH=), 7.74 (d, *J* = 8.8 Hz, 1H, H-6). ^{13}C NMR ($CDCl_3$) δ 18.2, 24.8, 55.7, 64.8, 64.0, 100.9, 107.8, 118.9, 122.5, 126.2, 127.8, 128.7, 132.8, 135.5, 141.9, 159.4, 160.4, 162.5, 190.1. ESI-MS (*m/z*): 353 (M + H); Anal. $C_{22}H_{24}O_4$ (C, H).

*5.3.23. (E)-3-(3,4-dimethoxyphenyl)-1-(2-methoxy-4-((3-methylbut-2-en-1-yl)oxy)phenyl)prop-2-en-1-one (**24**).* Starting from **34** (0.23 g, 1.0 mmol) and 3,4-dimethoxybenzaldheyde (0.18 g, 1.1 mmol) gave the crude final product **24** that was purified by flash chromatography (petroleum ether/EtOAc 4:1) and then crystallized from DCM/petroleum ether to obtain a yellow solid (0.29 g), 77% yield, mp 83-85 °C. ^{1}H NMR ($CDCl_3$) δ 1.78 (s, 3H, CH_3), 1.83 (s, 3H, CH_3), 3.90 (s, 6H, OCH_3), 3.93 (s, 3H, OCH_3), 4.59 (d, *J* = 7.4 Hz, 2H, OCH_2), 5.48-5.52 (m, 1H, CH), 6.54 (s, 1H, H-3), 6.58 (d, *J* = 8.4 Hz, 1H, H-5), 6.89 (d, *J* = 8.4 Hz, 1H, H-5'), 7.13 (d, *J* = 2.1, 1H, H-2'), 7.20 (dd, *J* = 8.4 and 2.1 Hz, 1H, H-6'), 7.37 (d, *J* = 15.6 Hz, 1H, =CH), 7.63 (d, *J* = 15.6 Hz, 1H, CH=), 7.73 (d, *J* = 8.8

602 Hz, 1H, H-6). ^{13}C NMR ($CDCl_3$) δ 18.2, 24.8, 55.7, 56.2, 64.8, 64.0, 100.9, 107.8, 118.5, 122.5,
603 125.3, 127.8, 132.1, 134.4, 141.9, 159.4, 160.4, 161.4, 162.5, 190.4. ESI-MS (*m/z*): 383 (M + H),
604 Anal. $C_{23}H_{26}O_5$ (C, H).

605 *5.3.24. (E)-1-(2-methoxy-4-(prop-2-yn-1-yloxy)phenyl)-3-(4-nitrophenyl)prop-2-en-1-one* ***(25)****.*
606 Starting from **36** (0.20 g, 1.0 mmol) and 4-nitrobenzaldheyde (0.17 g, 1.1 mmol) gave the crude
607 final product **25** that was purified by crystallization from ethanol to obtain a white solid (0.22 g),
608 67% yield, mp 178-180°C. ^{1}H NMR ($CDCl_3$) δ 2.59 (t, *J* = 2.4 Hz, 1H, C≡CH), 3.94 (s, 3H, OCH_3),
609 4.78 (d, *J* = 2.4 Hz, 2H, OCH_2), 6.61 (d, *J* = 2.0 Hz, 1H, H-3), 6.67 (dd, *J* = 2.0 and 8.4 Hz, 1H, H-
610 5), 7.64 (d, *J* = 16.0 Hz, 1H, =CH), 7.70 (d, *J* = 16.0 Hz, 1H, CH=), 7.73 (d, *J* = 8.4 Hz, 2H, H-2'
611 and H-6'), 7.82 (d, *J* = 8.4 Hz, 1H, H-6), 8.26 (d, *J* = 8.8 Hz, 2H, H-3' and H-5'). ^{13}C NMR
612 ($CDCl_3$) δ 55.7, 56.5, 77.7, 105.8, 121.3, 124.1, 128.6, 131.0, 133.2, 138.2, 160.7, 164.2, 183.2.
613 ESI-MS (*m/z*): 338 (M + H); Anal. $C_{19}H_{15}NO_5$ (C, H, N).

614 *5.3.25. (E)-1-(2,4-bis(prop-2-yn-1-yloxy)phenyl)-3-(4-nitrophenyl)prop-2-en-1-one* ***(26)****.* Starting
615 from **37** (0.23 g, 1.0 mmol) and 4-nitrobenzaldheyde (0.17 g, 1.1 mmol) gave the crude final
616 product **26** that was purified by flash chromatography (petroleum ether/EtOAc 9:1) and then
617 crystallized from ethanol to obtain a yellow solid (0.37 g), 95% yield, mp 186-188 °C. ^{1}H NMR
618 ($CDCl_3$) δ 2.58-2.60 (m, 2H, C≡CH), 4.75 (d, *J* = 2.4 Hz, 2H, OCH_2), 4.78 (d, *J* = 2.4 Hz, 2H,
619 OCH_2) 6.66 (d, *J* = 2.0 Hz, 1H, H-3), 6.70 (dd, *J* = 2.0 and 8.8 Hz, 1H, H-5), 7.60 (d, *J* = 15.6 Hz,
620 1H,=CH), 7.66 (d, *J* = 16 Hz, 1H, CH=), 7.74 (d, *J* = 8.8 Hz, 2H, H-2' and H-6'), 7.83 (d, *J* = 8.4
621 Hz, 1H, H-6), 8.23 (d, *J* = 8.8 Hz, 2H, H-3' and H-5'). ^{13}C NMR ($CDCl_3$) δ 55.7, 55.9, 76.2, 76.6,
622 77.7, 77.8, 101.8, 107.3, 123.1, 127.7, 130.5, 133.2, 138.2, 162.8, 164.4, 187.2. ESI-MS (*m/z*): 362
623 (M + H) Anal. $C_{21}H_{15}NO_5$ (C, H, N).

624 *5.3.26. (E)-1-(2-methoxy-4-(prop-2-yn-1-yloxy)phenyl)-3-(3,4,5-trimethoxyphenyl)prop-2-en-1-one*
625 ***(27)*** Starting from **36** (0.20 g, 1.0 mmol) and 3,4,5-trimethoxybenzaldheyde (0.21 g, 1.1 mmol)

gave the crude final product **27** that was purified by crystallization from EtOH to obtain a yellow solid (0.27 g), 73% yield, mp 106-108 °C. ^{1}H NMR ($CDCl_3$) δ 2.58 (s, 1H, C≡CH), 3.86 (s, 3H, OCH_3), 3.94 (s, 3H, OCH_3), 4.75 (d, *J* = 2.0 Hz, 2H, OCH_2), 6.65 (s, 1H, H-3), 6.67 (d, *J* = 8.4 Hz, 1H, H-5), 6.81 (s, 2H, H-3' e H-5'), 7.37 (d, *J* = 15.6 Hz, 1H, =CH), 7.58 (d, *J* = 8.8 Hz, 2H, H-2' and H-6'), 7.64 (d, *J* = 15.6 Hz, 1H, CH=), 7.78 (d, *J* = 8.8 Hz, 1H, H-6). ^{13}C NMR ($CDCl_3$) δ 55.8, 55.9, 56.0, 56.2, 56.3, 76.2, 76.6, 77.8. 77.9. 100.9, 107.8, 110.4, 118.5, 123.0, 123.6, 125.8, 131.0, 132.8, 142.5, 9 149.2, 157.8, 162.2, 190.5. ESI-MS (*m/z*): 382 (M + H); Anal. $C_{22}H_{22}O_6$ (C, H, N).

*5.3.27. (E)-3-(3,4-dimethoxyphenyl)-1-(2-methoxy-4-(prop-2-yn-1-yloxy)phenyl)prop-2-en-1-one (**28**).* Starting from **37** (0.23 g, 1.0 mmol) and 3,4-dimethoxybenzaldheyde (0.18 g, 1.1 mmol) gave the crude final product **28** that was purified by flash chromatography (petroleum ether/EtOAc 9:1) and then crystallized from EtOH to obtain a yellow solid (0.22 g), 69% yield, mp 130-132 °C. ^{1}H NMR ($CDCl_3$) δ 2.58 (s, 1H, C≡CH), 3.90 (s, 6H, OCH_3), 3.93 (s, 3H, OCH_3), 4.76 (s, 2H, OCH_2), 6.60 (s, 1H, H-3) 6.64 (d, *J* = 8.4 Hz, 1H, H-5), 6.88 (d, *J* = 8.4 Hz, 1H, H-5'), 7.12 (d, *J* = 2.2 Hz, 1H, H-2'), 7.19 (dd, *J* = 8.0 and 2.2 Hz, 1H, H-6'), 7.33 (d, *J* = 15.6 Hz, 1H, =CH), 7.62 (d, *J* = 15.6 Hz, 1H, CH=), 7.72 (d, *J* = 8.0 Hz, 1H, H-6). ^{13}C NMR ($CDCl_3$) δ 55.7, 55.8, 56.2, 56.5, 76.7, 77.9, 101.1, 107.1, 110.0, 111.4, 123.6, 123.9, 125.8, 127.3, 131.8, 142.7, 147.1, 154.5, 157.8, 161.4, 190.4. ESI-MS (*m/z*): 353 (M + H); Anal. $C_{21}H_{20}O_5$ (C, H).

*5.3.28. (E)-1-(2,4-bis(prop-2-yn-1-yloxy)phenyl)-3-(3,4,5-trimethoxyphenyl)prop-2-en-1-one (**29**).* Starting from **37** (0.23 g, 1 mmol) and 3,4,5-trimethoxybenzaldheyde (0.21 g, 1.1 mmol) gave the crude final product **29** that was purified by crystallization from ethanol to obtain a yellow solid (0.27 g), 67% yield, mp 147-138 °C. ^{1}H NMR ($CDCl_3$) δ 2.55-2.58 (m, 2H, C≡CH), 3.94 (s, 6H, OCH_3), 3.97 (s, 3H, OCH_3), 4.77-4.79 (m, 4H, OCH_2), 6.71 (d, *J* = 2.2 Hz, 1H, H-3) 6.88 (dd, *J* = 8.4 and 2.0 Hz, 1H, H-5), 6.81 (s, 2H, H-2' and H-6'), 7.42 (d, *J* = 15.6 Hz, 1H, =CH), 7.63 (d, *J* = 16.0 Hz, 1H, CH=), 7.81 (d, *J* = 8.8 Hz, 1H, H-6). ^{13}C NMR ($CDCl_3$) δ 55.8, 55.9, 56.0, 56.4, 56.5,

76.2, 76.7, 77.8, 77.9, 101.1, 107.1, 110.2, 111.3, 123.7, 125.4, 128.3, 132.5, 142.7, 149.1, 150.8, 151.1, 157.8, 161.4, 190.3. ESI-MS (*m/z*): 407 (M + H); Anal. $C_{24}H_{22}O_6$ (C, H).

*5.3.29. (E)-1-(2,4-bis(prop-2-yn-1-yloxy)phenyl)-3-(3,4-dimethoxyphenyl)prop-2-en-1-one (**30**).* Starting from **37** (0.23 g, 1.0 mmol) and 3,4-dimethoxybenzaldheyde (0.18 g, 1.1 mmol) gave the crude final product **30** that was purified by flash chromatography (petroleum ether/EtOAc 4:1) and then crystallized from EtOH to obtain a yellow solid (0.24 g), 65% yield, mp 137-139 °C. ^{1}H NMR ($CDCl_3$) δ 2.55-2.58 (m, 2H, C≡CH), 3.94 (s, 6H, OCH_3), 4.77-4.79 (m, 4H, OCH_2), 6.71 (d, *J* = 2.2 Hz, 1H, H-3) 6.88 (d, *J* = 8.4 and 2.2 Hz, 1H, H-5), 7.16 (d, *J* = 8.2 Hz, 1H, H-5'), 7.20 (d, *J* = 2.0 Hz, 1H,H-2'), 7.22 (dd, *J* = 8.0 and 2.2 Hz, 1H, H-6'), 7.40 (d, *J* = 15.6 Hz, 1H, =CH), 7.64 (d, *J* = 16.0 Hz, 1H, CH=), 7.75 (d, *J* = 8.8 Hz, 1H, H-6). ^{13}C NMR ($CDCl_3$) δ 55.8, 55.9, 56.0, 56.5, 76.2, 76.7, 77.8, 77.9, 101.1, 107.1, 110.0, 111.1, 122.9, 123.8, 125.1, 128.3, 132.6, 142.7, 149.1, 151.1, 157.8, 161.4, 190.4. ESI-MS (*m/z*): 377 (M + H); Anal. $C_{23}H_{20}O_5$ (C, H).

*5.3.30. (E)-1-(2,4-bis(prop-2-yn-1-yloxy)phenyl)-3-(4-methoxyphenyl)prop-2-en-1-one (**31**).* Starting from **37** (0.23 g, 1.0 mmol) and 4-methoxybenzaldheyde (0.14 g, 1.1 mmol) gave the crude final product **31** that was purified by flash chromatography (petroleum ether/EtOAc 9:1) and then crystallized from EtOH to obtain an orange solid (0.20 g), 59% yield; mp 120-122 °C. ^{1}H NMR ($CDCl_3$) δ 2.57-2.60 (m, 2H, C≡CH), 3.86 (s, 3H, OCH_3), 4.76 (d, *J* = 1.6 Hz, 2H, OCH_2), 4.78 (d, *J* = 2.0 Hz, 2H, OCH_2) 6.70 (d, *J* = 2.2 Hz, 1H, H-3), 6.72 (d, *J* = 8.2 Hz, 1H, H-5), 6.92 (d, *J* = 8.4 Hz, 2H, H-3' and H-5'), 7.42 (d, *J* = 15.6 Hz, 1H, =CH), 7.58 (d, *J* = 8.4 Hz, 2H, H-2' and H-6'), 7.66 (d, *J* = 15.6 Hz, 1H, CH=), 7.76 (d, *J* = 8.8 Hz, 1H, H-6). ^{13}C NMR ($CDCl_3$) δ 55.9, 56.0, 56.5, 76.2, 76.7, 77.7, 77.9, 101.1, 107.1, 110.0, 111.1, 122.4, 123.7, 125.2, 128.9, 132.7, 132.8, 142.7, 149.8, 157.8, 161.2, 190.5. ESI-MS (*m/z*): 345 (M + H); Anal. $C_{20}H_{15}NO_3$ (C, H, N).

*5.3.32. 2-cinnamoyl-5-((3-methylbut-2-en-1-yl)oxy)phenyl acetate (**20**).*Compound **19** (0.31 g, 1.0 mmol) was reacted with acetic anhydride (10 mL) and the mixture was heated under reflux for 4 hr

and then poured into ice/water. The solid was collected and crystallized from EtOH to give **19** as white solid (0.23 g), 66 % yield, mp 121-122 °C. ^{1}H NMR ($CDCl_3$) δ 1.79 (s, 3H, CH_3), 1.82 (s, 3H, CH_3), 2.35 (s, 3H, $COCH_3$), 4.56 (d, *J* = 6.0 Hz, 2H, OCH_2), 5.47-5.50 (m, 1H, =CH), 6.41 (d, *J* = 2.0, 1H, H-5), 6.60 (dd, *J* = 1.8 and 8.4 Hz, 1H, H-3), 7.27 (d, *J* = 15.6 Hz, 1H, =CH), 7.33-7.45 (m, 3H, H-3', H-4', H-5'), 7.53-7.61 (m, 2H, H-2'and H-6'), 7.65 (d, *J* = 15.3 Hz, 1H, =CH), 7.78 (d, *J* = 8.4 Hz, 1H, H-6). ^{13}C NMR ($CDCl_3$) δ 18.61, 20.5, 24.5, 65.1, 104.8, 118.6, 113.6, 118.6, 118.9, 120.5, 127.7, 128.2, 139.7, 135.9, 138.0, 145.2, 154.4, 154.7, 166.0, 169.11, 191.7. ESI-MS (*m/z*): 351 (M + H); Anal. $C_{20}H_{20}O_3$ (C, H).

5.4. Parasitology.

5.4.1. Parasites. Promastigote forms of a *L. donovani* reference strain (MHOM/NP/02/BPK282/0cl4), *L. major* reference strain (MHOM/SU/73/5-ASKH), *L. tropica* reference strain (MHOM/SU/74/K27), *L. infantum* reference strain (MHOM/ TN/ 80/ IPT1) were cultured at 26°C in HOMEM (Gibco Thermo Fisher Scientific Inc., Waltham, USA), a liquid custom made medium supplemented with 20% foetal bovine serum (FBS, EuroClone SpA, Milan, Italy) and 1% penicillin-streptomycin (EuroClone SpA).

5.4.2. Cell cultures. THP-1 cells (human leukemia monocytic cell line) were cultured at 37 °C in RPMI-1640 (EuroClone SpA) liquid medium supplemented with 10% FBS (EuroClone SpA), 1% levoglutamine (EuroClone SpA), Mercaptoethanol (Gibco) 50 µM , 1% penicillin-streptomycin. Vero cells (kidney of African green monkey epithelial cell line) were cultured at 37 °C in MEM liquid medium supplemented with 10% FBS (EuroClone SpA), 1% levoglutamine (EuroClone SpA), 1% penicillin-streptomycin (EuroClone SpA).

5.4.3. Promastigote growth inhibition assay. The late log/stationary phase of promastigotes were seeded with complete HOMEM medium at 10^6/mL in 96-well plates and incubated with tested compounds at a range concentration of 40 µM – 1.6 µM in a 26 °C incubator for 72 h. The antileishmanial drug amphotericin B was used as standard drug (positive control). Each experiment

699 was performed in duplicate. Stock solution of the compounds was 8 mM in DMSO. To estimate the
700 concentration at which the compounds caused 50% inhibition of growth (IC_{50}), the AlamarBlue
701 assay was employed (Life Technologies, Thermo Fisher Scientific Inc., Waltham, USA). The
702 AlamarBlue assay includes a colorimetric growth indicator based on detection of metabolic activity.
703 Specifically, the system incorporates an oxidation-reduction (REDOX) indicator that fluoresces and
704 changes color in response to chemical reduction of growth medium resulting from cell growth: the
705 method monitors the reducing environment of proliferating cells; the cell permeable resazurin is
706 added (nonfluorescent form, blue color) and, upon entering cells, is reduced to resorufin
707 (fluorescent form, red color) as result of cellular metabolic activity. Evaluation was performed by
708 adding 20 µL of AlamarBlue and incubating at 26 °C for 24 h. The reducing environment was
709 evaluated after 24 hours by absorbance measurement at the Multiskan Ascent Plate Reader (Thermo
710 Fisher Scientific Inc.) at 550 nm and 630 nm.
711 *5.4.4. Antiamastigote assay*. Human acute monocytic leukemia cell line (THP1) were infected with
712 *L. donovani* promastigotes for the assessment of the activity of compounds against the amastigote
713 form of *Leishmania* parasite. Cells were seeded in a 96-well plate (10^5 cells/mL) in complete
714 RPMI-1640 medium and PMA (0.1 µM, Cayman Chemical Company, Ann Arbor, Michigan, USA)
715 was added for the cells adherence. Cells were incubated at 37 °C in a 5% CO_2 incubator. After 48 h,
716 the medium was replaced with fresh medium containing stationary phase promastigotes that were
717 then phagocytized by monocytic cells and transformed into intracellular amastigotes. After 24 h of
718 incubation, chalcone compounds were added and the plates were incubated at 37°C in a 5% CO_2
719 incubator for 72 h. After incubation, wells were washed, fixed, and stained with Giemsa. Staining
720 was detected using a Nikon Eclipse E200 light microscope (Nikon, Tokyo, Japan). The infectivity
721 index (% of infected macrophages x average number of amastigotes per macrophage) was
722 determined by counting at least 100 cells in duplicate cultures.
723 *5.4.5. Citotoxicity test.* Mammalian kidney epithelial cells (Vero cell line) were seeded (10^5/mL)
724 with complete MEM medium in 96-well plates and incubated with test compounds up to a

concentration of 600µM at 37 °C in a 5% CO_2 incubator. Similarly, THP1 were seeded in a 96-well plate (10^5 cells/mL) in complete RPMI-1640 medium and PMA (0.1 µM) was added for the cells adherence. After 72 h of incubation, 20 µL of AlamarBlue reagent was added to each well and incubated at 37 °C for 24 h. Reduction of resazurin to resorufin was evaluated after 24 h by absorbance measurement at the Multiskan Ascent Plate Reader (Thermo Fisher Scientific Inc.,) at 550 nm and 630 nm. DMSO was also tested on *Leishmania* promastigotes and no toxicity was detected. Thus, DMSO did not influence the toxicity of the compounds. Each experiment was performed in duplicate. The selectivity index (SI) for each compound was calculated as the ratio between cytotoxicity (CC_{50}/72h) in Vero cells and activity (IC_{50}/72h) against *Leishmania* promastigotes.

5.5. Surface Plasmon Resonance (SPR) measurements

SPR experiments were carried out using a SensiQ Pioneer system (SensiQ, ICxNomadics Inc.).

The sensor chips (COOH5 SensiQ) were chemically activated by injection of 250 µl of a 1:1 mixture of N-hydroxysuccinimide (50 mM) and N-ethyl-N-(3-dimethylaminopropyl)carbodiimide (200 mM) at a flow rate of 25 µl/min. Recombinant *Li*TR was immobilized on the activated sensor chip via amine coupling. The reaction was carried out at a rate of 10 mL/min in 20 mM sodium acetate at pH 4.5; the remaining N-hydroxysuccinimide esters were blocked by injecting 100 µL of 1 M ethanolamine hydrochloride. Recombinant *Li*TR was captured to approximately 2000 RU. The chalcone compounds (analytes) were dissolved at a concentration of 10 mM or 20 mM in dimethylsulfoxide (DMSO), and diluted 1:100 in HEPES-buffered saline (HBS: 10 mM HEPES, pH 7.4; 150 mM NaCl; 0.005 % surfactant P20).

FastStep injections of samples (100 µM analytes in HBS + 1% DMSO), and reference buffer (HBS + 1% DMSO) were performed: either the inhibitor and reference buffer were automatically diluted in HBS and injected by 7 serial doubling steps (step contact time = 15 s, nominal flow rate = 200 µl/min). The following analytes were injected: 0-17 s: analyte concentration=1.56 µM; 17-33 s: 3.12 µM; 33-48 s: 6.25 µM; 48-62 s: 12.5 µM; 63-78 s: 25 µM; 78-93 s: 50 µM; 94-100 s: 100 µM;

for each injection, a maximal RU value was obtained. In control experiments, the sensor chip was treated as described above in the absence of immobilized protein. The interaction of the immobilized protein with the analytes was detected by mass concentration dependent changes of the refractive index on the sensor chip surface. The changes in the observed SPR signal are expressed as Resonance Units (RU). Typically, a response change of 1000 RU corresponds to a change in the surface concentration on the sensor chip of about 1 ng of protein per mm^2. The increase in RU relative to baseline indicates complex formation between the immobilized protein and the analytes. For each concentration, the plateau region represents the steady-state phase of the interaction. The decrease in RU after 100 s indicates analyte dissociation from the immobilized ligand after buffer injection.

Each sensorgram is the average of three different experiments. Sensorgrams were subjected to global analysis using QDat software 2.2.0.23; for each analyte concentration a % Response was calculated, allowing a local Rmax fit (according to the molecular weight of each compound) and displaying as a response relative to the Rmax. % Response vs. analyte concentration was plotted, and K_D values were calculated for each analyte both from Scatchard plots and from global analysis using the QDat software, by fitting a simple 1:1 binding model to the data.

5.6. Enzymatic assay

*Li*TR was cloned and purified as previously described by Baiocco et al. [13] [35]. Enzyme inhibition assays were carried out at 25 °C using a diode array Hewlett–Packard HP8452A spectrophotometer. The solution containing TR 40 nM, TS_2 (75 μM, 100 μM, 200 μM, 400 μM) and chalcone compound **6** (30 nM, 50 nM, 70 nM, 1 μM) were allowed to equilibrate for 2 min in a quartz cuvette. Assays were initiated by addition of NADPH 40 μM and the absorbance decrease at 340 nm, which indicates the oxidation of NADPH, was followed. The concentrations of NADPH was calculated using the molar extinction coefficient $\varepsilon = 6{,}222\ M^{-1}\ cm^{-1}$ at 340 nm. Trypanothione disulfide (Bachem) and NADPH (Sigma) were used for the experiments.

5.7. Docking experiments

The pdb coordinates of Compound **6** were designed using the WebGL server [36]. Docking calculations were performed by the Autodock 4.0 software [37]. Docking procedures were performed using the structures of TR in both the oxidized form (PDB code: 2JK6) and the reduced form (PDB code 4ADW) downloaded from the protein data bank (PDB code: 2JK6). The TR structure was edited using the software from the ADT package to remove all water molecules and add hydrogen atoms. Non-polar hydrogens and lone pairs were then merged and each atom within the macromolecule was assigned a Gasteiger partial charge. A grid box of 80 × 80 × 80 points, with a spacing of 0.375 Å, was positioned at the active-site gorge. The Lamarckian genetic algorithm (LGA) was employed with the maximum number of generations and energy evaluations of 631 and 1000334, respectively.

Acknowledgments

This work was supported by Fondazione Del Monte di Bologna e Ravenna (Prot. Nr. 349 bis/2016), by the University of Bologna (RFO funds) and by the Ministry of Education (PRIN 2015, Prot. 20154JRJPP). We would like to thank Dr. David Staid for his help to conceive the docking experiments.

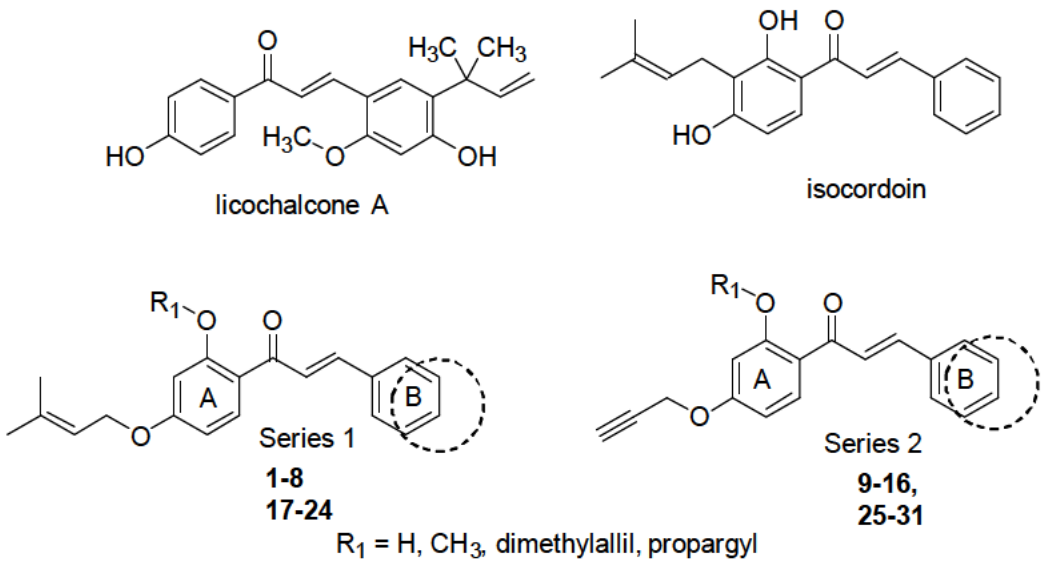

795

796 **Figure 1.** Structures of licochalcone A, isocordoin and general structure of the newly synthesized
797 compounds (Series 1 and 2).

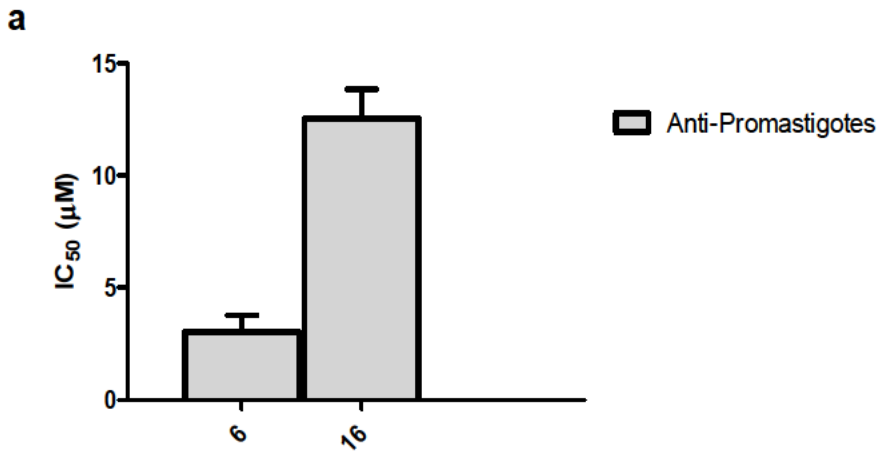

798

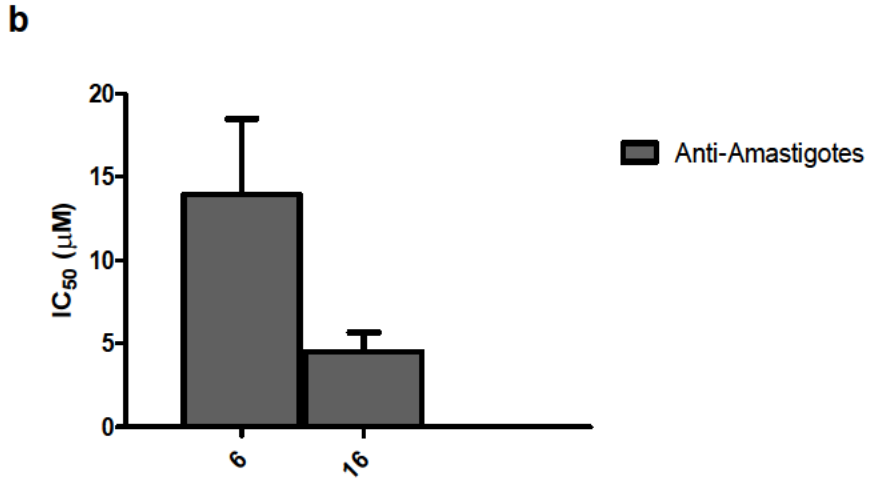

799

800 **Figure 2.** Antipromastigote (2a) and antiamastigote (2b) activity of compound **6** and compound **16.**
801 *L. donovani* promastigotes were treated with tested compounds at a concentration range of 40 - 1.5
802 µM for 72 h, then the effect of the chalcones was evaluated by the AlamarBlue® assay. For the
803 amastigote assay, *Leishmania*-infected THP-1 cells were treated with tested compounds at a

concentration range of 40-1.5 µM for 72h, then fixed and stained with Giemsa. Results from three independent experiments performed in duplicates are shown. IC_{50}/72h, as concentration of compound required to inhibit growth by 50%, is plotted in y axis. Bars represent mean values ± standard errors.

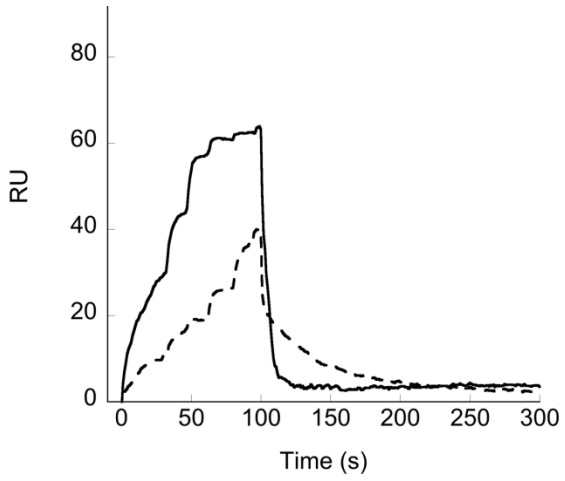

Figure 3. SPR binding curves (sensorgrams) obtained by injecting different concentrations (range 1.5-100 µM) of compounds **6** (full line) and **16** (dashed line) on a surface of covalently immobilized TR; dissociations phases are also shown. RU; response units.

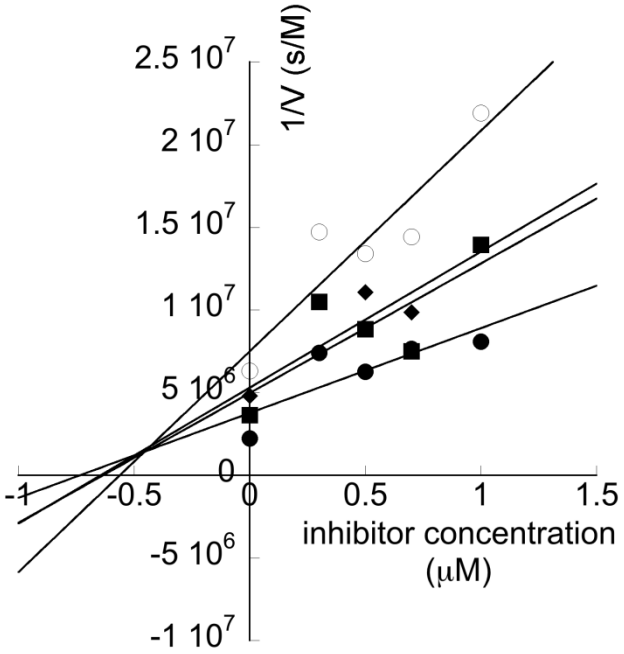

Figure 4 Dixon plot of TR inhibition by compound **6** (concentration range**:** 0-1.0 µM**).** Open circles [TS_2] = 75 µM; filled squares [TS_2] = 100 µM; filled diamonds [TS_2] = 200 µM and filled circles [TS_2] = 400 µM.

a

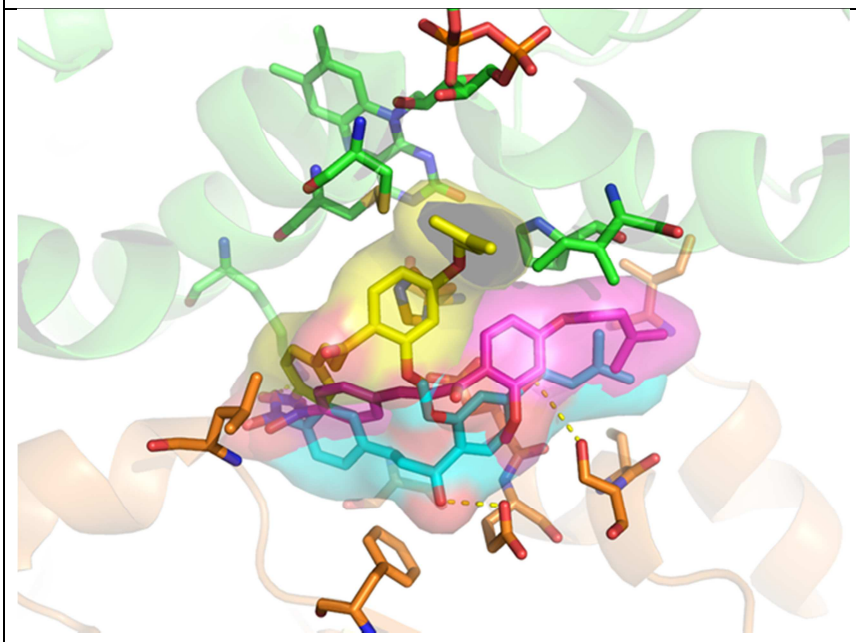

b

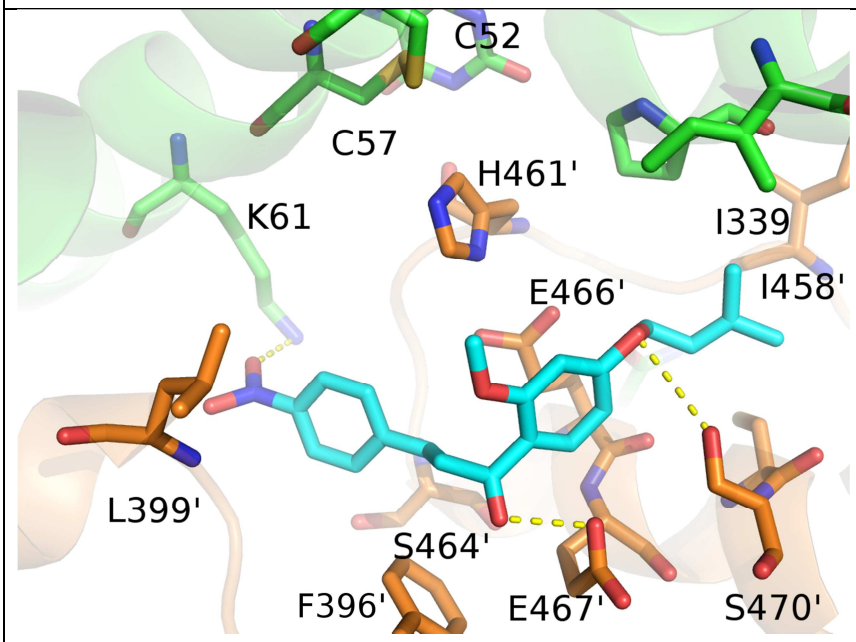

c

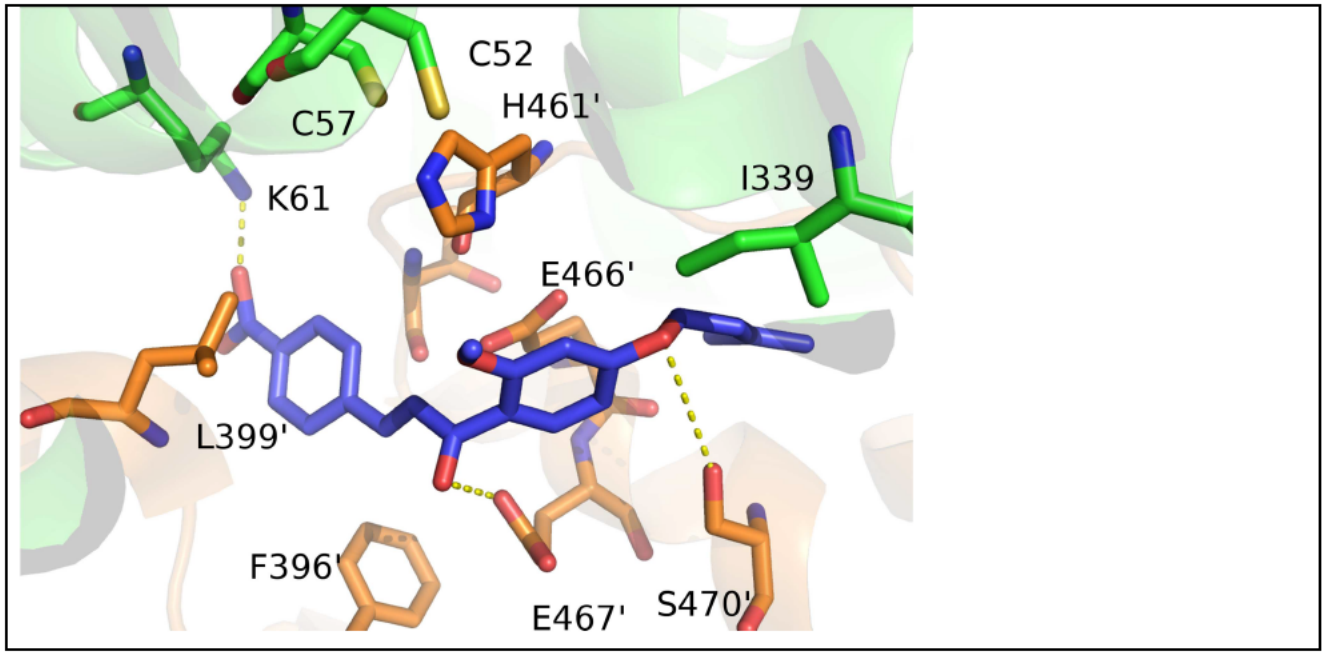

Figure 5. Blow up of the complex between compound **6** and TR obtained by docking experiments using both the oxidized form (PDB code: 2JK6) (a and b) and the reduced form (PDB code 4ADW) (c) of the protein. **a**. In A are represented the lowest energy poses belonging to the most populated clusters (reported in TableS1). The pose 3 belonging to cluster 1 is colored pink; the pose 60 belonging to cluster 2 is colored cyan; the pose 94 belonging to cluster 3 is colored yellow. **b.** In b, the pose of compound **6** docked in the oxidized form of TR belonging to the most populated cluster (pose 60 belonging to cluster 2) is represented. **c.** In c, the pose of compound **6** docked in the reduced form of TR belonging to the most populated cluster (pose 61 belonging to cluster 3) is represented. Compound **6** and the residues interacting with it are indicated and represented as sticks. The two TR subunits are colored in green and orange whereas compound **6** docked in the oxidized TR is colored cyan and compound **6** docked in reduced TR is colored blue. The picture was obtained using PyMOL (The PyMOL Molecular Graphics System, Version 2.0 Schrödinger, LLC.)

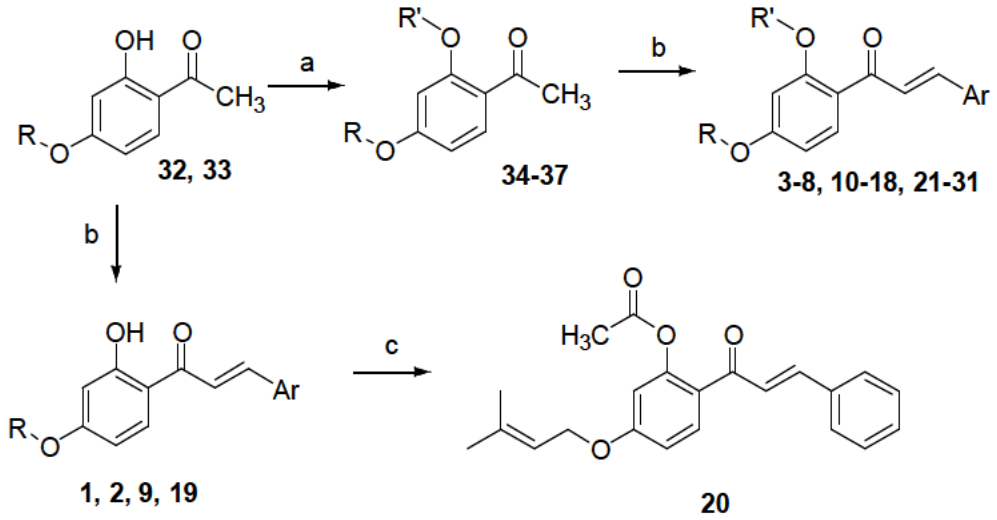

Scheme 1. Synthetic route of compounds **1-37**[a]

[a]Reagents and conditions: a) selected alkyl bromide, K_2CO_3, acetone, reflux; b) KOH 50%, EtOH, rt, 18 h; c) acetic anhydride, reflux.

838 **Table 1.** Inhibitory activity of chalcones **1-31** against promastigotes of *L. donovani* growth,
839 cytotoxicity in mammalian kidney epithelial cells and in a human monocytic cell line and selectivity
840 indexes.

Comp	Structure	*L.donov* IC_{50} (μM)[a]	Vero CC_{50} (μM)[b]	SI[c,d]	THP-1 CC_{50} (μM)	SI[c, e]
1	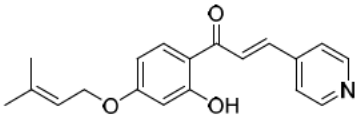	5.0	40.0	8	16.0	3.2
2	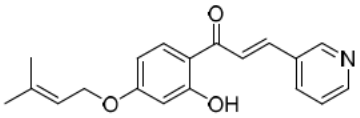	8.5	210.0	24.7	100.0	11.8
3	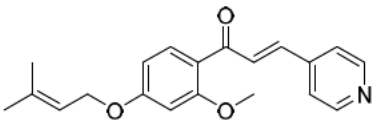	10.5	16.0	1.5	16.0	1.5
4	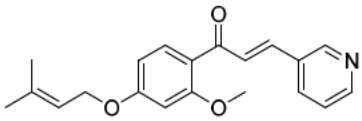	10.5	22.0	2	40.0	3.8
5	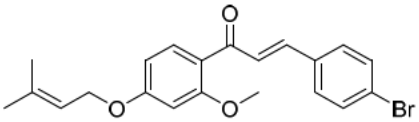	16.0	600.0	37.5	100.0	6.3
6	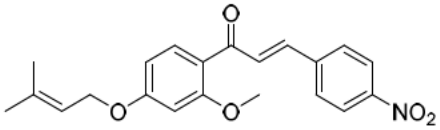	3.0	600.0	200	600.0	200
7	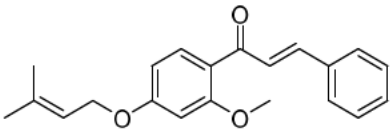	15.0	50.0	3.3	50.0	3.3
8	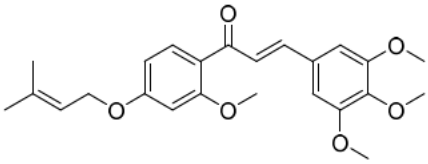	11.0	40.0	3.6	25.0	2.3
9	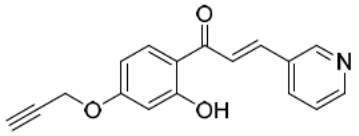	17.5	40.0	2.3	25.0	1.4
10	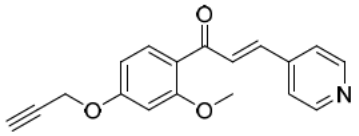	4.0	20.0	5	16.0	4
11	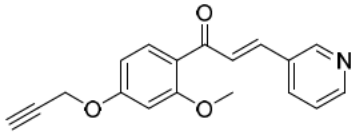	9.5	15.0	1.6	16.0	1.7

12	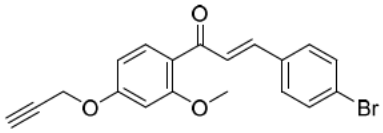	21.5	100.0	4.6	100.0	4.6
13	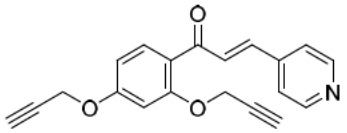	7.0	10.0	1.4	11.0	1.6
14	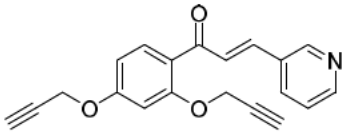	4.0	6.0	1.5	15	3.8
15	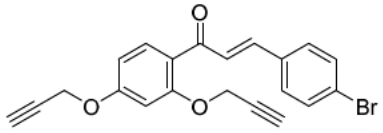	15.0	420.0	28	25.0	1.6
16	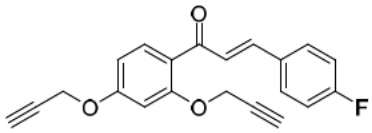	12.5	600.0	48	600.0	48
17	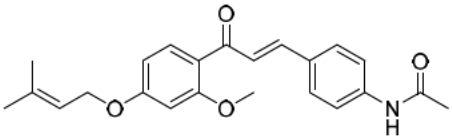	n.i.	n.d.	n.d.	n.d.	n.d.
18	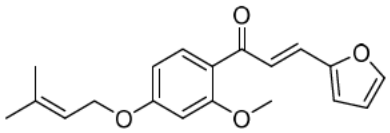	n.i.	n.d.	n.d.	n.d.	n.d.
19	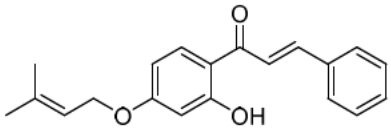	n.i.	n.d.	n.d.	n.d.	n.d.
20	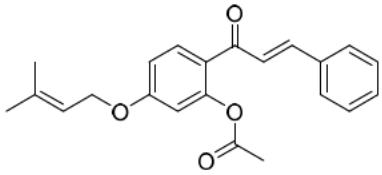	n.i.	n.d.	n.d.	n.d.	n.d.
21	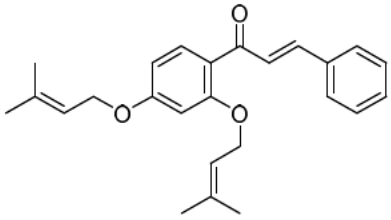	n.i.	n.d.	n.d.	n.d.	n.d.
22	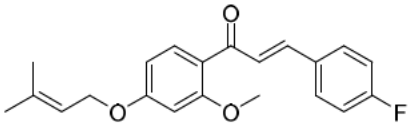	n.i.	n.d.	n.d.	n.d.	n.d.
23	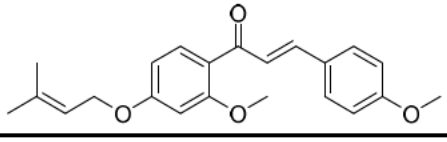	n.i.	n.d.	n.d.	n.d.	n.d.

24	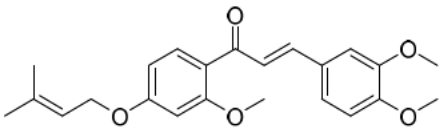	n.i.	n.d.	n.d.	n.d.	n.d.
25	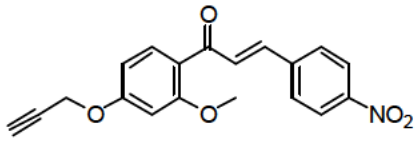	n.i.	n.d.	n.d.	n.d.	n.d.
26	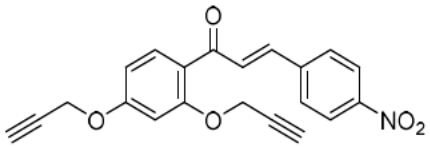	n.i.	n.d.	n.d.	n.d.	n.d.
27	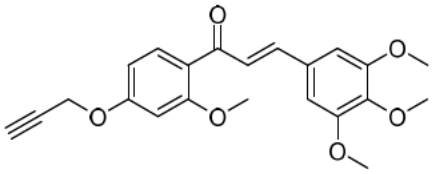	n.i.	n.d.	n.d.	n.d.	n.d.
28	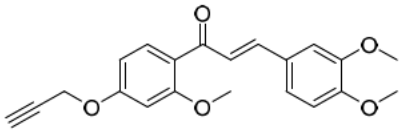	n.i.	n.d.	n.d.	n.d.	n.d.
29	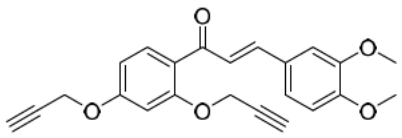	n.i.	n.d.	n.d.	n.d.	n.d.
30	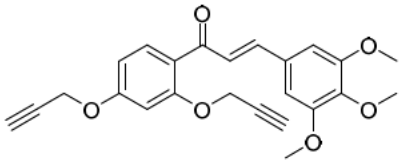	n.i.	n.d.	n.d.	n.d.	n.d.
31	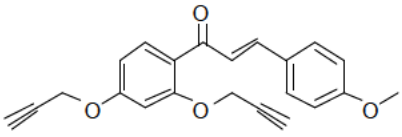	n.i.	n.d.	n.d.	n.d.	n.d.
Amph B		0.3	200.0	666	200.0	666

[a]IC_{50}/72h represents concentration of a compound that causes 50% growth inhibition and is the mean of two independent determinations. The experimental error was within 50%. [b] CC_{50}/72h represents 50% cytotoxic concentration. [c]SI; Selectivity index (SI = CC_{50}/IC_{50}). [d]SI was calculated considering CC_{50} on Vero cells. [e]SI was calculated considering CC_{50} on THP1 cells. Comp; compounds. n.i.; not inhibiting parasite growth up to 40 µM. n.d.; not determined due to the low antileishmanial potency. Amph B; amphotericin B.

References

[1] D. Pace, Leishmaniasis, J. Infect., 69 Suppl 1 (2014) S10-18.

[2] WHO, Control of the leishmaniases: report of a meeting of the WHO Expert Committee on the Control of Leishmaniases, Geneva, 22-26 March 2010, in: WHO technical report series, 2010.

[3] D. Savoia, Recent updates and perspectives on leishmaniasis, J. Infect. Dev. Ctries, 9 (2015) 588-596.

[4] P.J. Hotez, B. Pecoul, "Manifesto" for advancing the control and elimination of neglected tropical diseases, PLoS Negl. Trop. Dis., 4 (2010) e718.

[5] J.F. Barbosa, S.M. de Figueiredo, F.M. Monteiro, F. Rocha-Silva, C. Gaciele-Melo, S.S. Coelho, S. Lyon, R.B. Caligiorne, New Approaches on Leishmaniasis Treatment and Prevention: A Review of Recent Patents, Recent Pat. Endocr. Metab. Immune Drug Discov., 9 (2015) 90-102.

[6] R.K. Jha, A.K. Sah, D.K. Shah, P. Sah, The treatment of visceral leishmaniasis: safety and efficacy, JNMA J. Nepal Med. Assoc., 52 (2013) 645-651.

[7] D. Smirlis, M.B. Soares, Selection of molecular targets for drug development against trypanosomatids, Sub-cellular biochemistry, 74 (2014) 43-76.

[8] S. Muller, E. Liebau, R.D. Walter, R.L. Krauth-Siegel, Thiol-based redox metabolism of protozoan parasites, Trends in parasitology, 19 (2003) 320-328.

[9] K. Augustyns, K. Amssoms, A. Yamani, P.K. Rajan, A. Haemers, Trypanothione as a target in the design of antitrypanosomal and antileishmanial agents, Curr. Pharm. Des., 7 (2001) 1117-1141.

[10] A. Ilari, A. Fiorillo, P. Baiocco, E. Poser, G. Angiulli, G. Colotti, Targeting polyamine metabolism for finding new drugs against leishmaniasis: a review, Mini Rev. Med. Chem., 15 (2015) 243-252.

[11] L.R. Krauth-Siegel, M.A. Comini, T. Schlecker, The trypanothione system, Sub-cellular biochemistry, 44 (2007) 231-251.

[12] A. Ilari, A. Fiorillo, I. Genovese, G. Colotti, Polyamine-trypanothione pathway: an update, Future Med. Chem., 9 (2017) 61-77.

[13] P. Baiocco, G. Colotti, S. Franceschini, A. Ilari, Molecular Basis of Antimony Treatment in Leishmaniasis, J. Med. Chem., 52 (2009) 2603-2612.

[14] P. Baiocco, A. Ilari, P. Ceci, S. Orsini, M. Gramiccia, T. Di Muccio, G. Colotti, Inhibitory Effect of Silver Nanoparticles on Trypanothione Reductase Activity and Leishmania infantum Proliferation, ACS Med. Chem. Lett., 2 (2011) 230-233.

[15] A. Ilari, P. Baiocco, L. Messori, A. Fiorillo, A. Boffi, M. Gramiccia, T. Di Muccio, G. Colotti, A gold-containing drug against parasitic polyamine metabolism: the X-ray structure of trypanothione reductase from Leishmania infantum in complex with auranofin reveals a dual mechanism of enzyme inhibition, Amino acids, 42 (2012) 803-811.

[16] G. Colotti, A. Ilari, A. Fiorillo, P. Baiocco, M.A. Cinellu, L. Maiore, F. Scaletti, C. Gabbiani, L. Messori, Metal-based compounds as prospective antileishmanial agents: inhibition of trypanothione reductase by selected gold complexes, ChemMedChem, 8 (2013) 1634-1637.

[17] P. Baiocco, G. Poce, S. Alfonso, M. Cocozza, G.C. Porretta, G. Colotti, M. Biava, F. Moraca, M. Botta, V. Yardley, A. Fiorillo, A. Lantella, F. Malatesta, A. Ilari, Inhibition of Leishmania infantum trypanothione reductase by azole-based compounds: a comparative analysis with its physiological substrate by X-ray crystallography, ChemMedChem, 8 (2013) 1175-1183.

[18] F. Saccoliti, G. Angiulli, G. Pupo, L. Pescatori, V.N. Madia, A. Messore, G. Colotti, A. Fiorillo, L. Scipione, M. Gramiccia, T. Di Muccio, R. Di Santo, R. Costi, A. Ilari, Inhibition of Leishmania infantum trypanothione reductase by diaryl sulfide derivatives, J. Enzyme Inhib. Med. Chem., 32 (2017) 304-310.

[19] I.A. Rodrigues, A.M. Mazotto, V. Cardoso, R.L. Alves, A.C. Amaral, J.R. Silva, A.S. Pinheiro, A.B. Vermelho, Natural Products: Insights into Leishmaniasis Inflammatory Response, Mediators Inflamm., 2015 (2015) 835910.

[20] A. Oryan, Plant-derived compounds in treatment of leishmaniasis, Iran J. Vet. Res., 16 (2015) 1-19.
[21] B.E. Evans, K.E. Rittle, M.G. Bock, R.M. DiPardo, R.M. Freidinger, W.L. Whitter, G.F. Lundell, D.F. Veber, P.S. Anderson, R.S. Chang, et al., Methods for drug discovery: development of potent, selective, orally effective cholecystokinin antagonists, J. Med. Chem., 31 (1988) 2235-2246.
[22] N.K. Sahu, S.S. Balbhadra, J. Choudhary, D.V. Kohli, Exploring pharmacological significance of chalcone scaffold: a review, Curr. Med. Chem., 19 (2012) 209-225.
[23] J.R. Dimmock, D.W. Elias, M.A. Beazely, N.M. Kandepu, Bioactivities of chalcones, Curr. Med. Chem., 6 (1999) 1125-1149.
[24] M. Liu, P. Wilairat, S.L. Croft, A.L. Tan, M.L. Go, Structure-activity relationships of antileishmanial and antimalarial chalcones, Bioorg. Med. Chem., 11 (2003) 2729-2738.
[25] R. Shivahare, V. Korthikunta, H. Chandasana, M.K. Suthar, P. Agnihotri, P. Vishwakarma, T.K. Chaitanya, P. Kancharla, T. Khaliq, S. Gupta, R.S. Bhatta, J.V. Pratap, J.K. Saxena, S. Gupta, N. Tadigoppula, Synthesis, structure-activity relationships, and biological studies of chromenochalcones as potential antileishmanial agents, J. Med. Chem., 57 (2014) 3342-3357.
[26] R. Borges-Argaez, T. Vela-Catzin, A. Yam-Puc, M.J. Chan-Bacab, R.E. Moo-Puc, M. Caceres-Farfan, Antiprotozoal and Cytotoxic Studies on Some Isocordoin Derivatives, Planta Med, 75 (2009) 1336-1338.
[27] H. Hussain, A. Al-Harrasi, A. Al-Rawahi, I.R. Green, S. Gibbons, Fruitful decade for antileishmanial compounds from 2002 to late 2011, Chem. Rev., 114 (2014) 10369-10428.
[28] N. Singh, B.B. Mishra, S. Bajpai, R.K. Singh, V.K. Tiwari, Natural product based leads to fight against leishmaniasis, Bioorg. Med. Chem., 22 (2014) 18-45.
[29] S. Gupta, R. Shivahare, V. Korthikunta, R. Singh, N. Tadigoppula, Synthesis and biological evaluation of chalcones as potential antileishmanial agents, Eur. J. Med. Chem., 81 (2014) 359-366.
[30] P. Boeck, C.A. Bandeira Falcão, P.C. Leal, R.A. Yunes, V.C. Filho, E.C. Torres-Santos, B. Rossi-Bergmann, Synthesis of chalcone analogues with increased antileishmanial activity, Bioorg. Med. Chem., 14 (2006) 1538-1545.
[31] E.C. Torres-Santos, M.I. Sampaio-Santos, F.S. Buckner, K. Yokoyama, M. Gelb, J.A. Urbina, B. Rossi-Bergmann, Altered sterol profile induced in Leishmania amazonensis by a natural dihydroxymethoxylated chalcone, J. Antimicrob. Chemother., 63 (2009) 469-472.
[32] M. Chen, S.B. Christensen, T.G. Theander, A. Kharazmi, Antileishmanial activity of licochalcone A in mice infected with Leishmania major and in hamsters infected with Leishmania donovani, Antimicrob. Agents Chemother., 38 (1994) 1339-1344.
[33] S. Krieger, W. Schwarz, M.R. Ariyanayagam, A.H. Fairlamb, R.L. Krauth-Siegel, C. Clayton, Trypanosomes lacking trypanothione reductase are avirulent and show increased sensitivity to oxidative stress, Mol. Microbiol., 35 (2000) 542-552.
[34] M.C. do Nascimento, W.B. Mors, Chalcones of the root bark of Derris sericea, Phytochemistry, 11 (1972) 3023-3028.
[35] P. Baiocco, S. Franceschini, A. Ilari, G. Colotti, Trypanothione reductase from Leishmania infantum: cloning, expression, purification, crystallization and preliminary X-ray data analysis, Protein Pept. Lett., 16 (2009) 196-200.
[36] S. Yuan, H.C.S. Chan, Z. Hu, Implementing WebGL and HTML5 in Macromolecular Visualization and Modern Computer-Aided Drug Design, Trends in biotechnology, 35 (2017) 559-571.
[37] G.M. Morris, R. Huey, W. Lindstrom, M.F. Sanner, R.K. Belew, D.S. Goodsell, A.J. Olson, AutoDock4 and AutoDockTools4: Automated docking with selective receptor flexibility, Journal of computational chemistry, 30 (2009) 2785-2791.

- The development of new, effective and safe antileishmanial drugs is urgently needed.
- The enzyme trypanothione reductase, by disrupting *Leishmania* parasite redox balance. represents a validated molecular target for the development of antiparasitic agents.
- Chalcone as useful template for the design of novel antileishmanial compounds.
- 16 of the newly synthetized chalcones were active against *L.donovani in vitro.*
- Chalcone **6** potently inhibits leishmanial trypanothione reductase.